

AD 748812

RADC-TR-72-178  
Final Technical Report  
July 1972



METRIC CALIBRATION OF THE AERIAL PHOTOGRAPHIC SYSTEM  
BY THE METHOD OF MIXED RANGES

The Ohio State University Research Foundation

Approved for public release;  
distribution unlimited.

Reproduced by  
NATIONAL TECHNICAL  
INFORMATION SERVICE  
U S Department of Commerce  
Springfield VA 22151

Rome Air Development Center  
Air Force Systems Command  
Griffiss Air Force Base, New York

DDC  
RECEIVED  
SEP 28 1972  
REGULATED  
B

## DOCUMENT CONTROL DATA - R &amp; D

(Security classification of title, body of abstract and indexing annotation must be entered when the overall report is classified)

1. ORIGINATING ACTIVITY (Corporate author) The Ohio State University Research Foundation Dept. of Geodetic Science Columbus, Ohio 43212		2a. REPORT SECURITY CLASSIFICATION Unclassified	
		2b. GROUP N/A	
3. REPORT TITLE METRIC CALIBRATION OF THE AERIAL PHOTOGRAPHIC SYSTEM BY THE METHOD OF MIXED RANGES			
4. DESCRIPTIVE NOTES (Type of report and inclusive dates) Final Report 4/16/71 - 4/14/72			
5. AUTHOR(S) (First name, middle initial, last name) Dr. Dean C. Merchant			
6. REPORT DATE July 1972	7a. TOTAL NO. OF PAGES 80	7b. NO. OF REFS 19	
8a. CONTRACT OR GRANT NO. F30602-71-C-0249 Job Order No. 60350111		8b. ORIGINATOR'S REPORT NUMBER(S) Dept. of Geodetic Science Report No. 172	
		8c. OTHER REPORT NO(S) (Any other numbers that may be assigned this report) RADC-TR-72-178	
10. DISTRIBUTION STATEMENT Approved for public release; distribution unlimited.			
11. SUPPLEMENTARY NOTES None		12. SPONSORING MILITARY ACTIVITY Rome Air Development Center (IRAG) Griffiss Air Force Base, New York 13440	
13. ABSTRACT A new procedure for the calibration of the aerial photographic system is described and the results of a live data demonstration are reported. The procedure, termed the Method of Mixed Ranges (MMR), utilizes a three-dimensional targeted control range simultaneously with a conventional level range in an adjustment in which the elements of interior orientation are carried as common parameters for all exposures. The use of the three-dimensional range for suppressing high correlations between certain elements of interior and exterior orientation is thought to be unique for the normal aerial case. The advantage of the MMR procedure is in the fact that no modification to the total operational photographic system is required. The only exception is in the choice of the conditional function which then includes parameters of interior orientation.  This report describes the theory and results of the application of the MMR procedure to the Casa Grande and Mt. Graham ranges located in Arizona. Ten photographs were simultaneously adjusted. The rms error of photo coordinate-residuals after adjustment was 5.1 micrometers determined from 250 coordinate observations. The conclusion is that the MMR offers a cost-effective procedure for the calibration of the aerial photographic system.			

UNCLASSIFIED

Security Classification

14 . KEY WORDS	LINK A		LINK B		LINK C	
	ROLE	WT	ROLE	WT	ROLE	WT
Photogrammetry						
Aerial Cameras						
Mapping						
Camera Calibration						

UNCLASSIFIED

Security Classification

**METRIC CALIBRATION OF THE AERIAL PHOTOGRAPHIC SYSTEM  
BY THE METHOD OF MIXED RANGES**

**Dr. Dean C. Merchant**

**The Ohio State University Research Foundation**

**Approved for public release;  
distribution unlimited.**

FOREWORD

This final report was prepared by Dr. Dean C. Merchant, Associate Professor and Project Supervisor in the Department of Geodetic Science, The Ohio State University Research Foundation, under contract F30602-71-C-0249, Job Order Number 60350111. This contract was administered by Rome Air Development Center, Griffiss Air Force Base, New York, with Mr. John R. Callander (IRAG) as the Project Engineer.

This report, Department of Geodetic Science Number 172, covers research between 16 April 1971 and 14 April 1972.

This document has been reviewed by the Information Office (OI) and is releasable to the National Technical Information Service.

This technical report has been reviewed and is approved.

*John R. Callander*

Approved: JOHN R. CALLANDER  
Project Engineer

*Howard Davis*

Approved: FRANZ H. DETTMER  
Colonel, USAF  
Chief, Intel & Recon Division

FOR THE COMMANDER:

*Fred I. Diamond*

FRED I. DIAMOND  
Acting Chief, Plans Office

## ABSTRACT


A new procedure for the calibration of the aerial photographic system is described and the results of a live data demonstration are reported. The procedure, termed the Method of Mixed Ranges (MMR), utilizes a three-dimensional targeted control range simultaneously with a conventional level range in an adjustment in which the elements of interior orientation are carried as common parameters for all exposures. The use of the three-dimensional range for suppressing high correlations between certain elements of interior and exterior orientation is thought to be unique for the normal aerial case. The advantage of the MMR procedure is in the fact that no modification to the total operational photographic system is required. The only exception is in the choice of the conditional function which then includes parameters of interior orientation.

This report describes the theory and results of the application of the MMR procedure to the Casa Grande and Mt. Graham ranges located in Arizona. Ten photographs were simultaneously adjusted. The rms error of photo coordinate-residuals after adjustment was  $5.1 \mu\text{m}$  determined from 250 coordinate observations. The conclusion is that the MMR offers a cost-effective procedure for the calibration of the aerial photographic system.

## EVALUATION MEMO

While previously relying upon laboratory calibration procedures, the photogrammetric community has long recognized the merits of calibration of the aerial camera system within its intended environment. This has been demonstrated but heretofore has relied upon some external means of determining the position of the camera at the instant of exposure. Precise electronic distance measuring equipment and/or ballistic cameras have been used but these are extremely expensive to operate and usually require some modification to the aircraft. Ideally, no modifications to either the aircraft or the camera are desired together with the elimination of external tracking requirements. The method of mixed ranges (MMR) outlined in this report demonstrates such a procedure.

Of specific interest to the USAF is the application of this technique to reconnaissance cameras employed in high performance aircraft. With no modifications required to the aircraft, a range, once established, would afford a means of calibration which would be economically sound and requiring little time expenditure to accomplish the calibration task. The task, described in this report, was accomplished using a precise mapping camera to serve as an experimental control. These results are extremely encouraging and future work will concentrate upon the application to the non-metric camera. Such work is in direct pursuance of RADC TPO-5.

  
JOHN R. CALLANDER  
Project Engineer

## TABLE OF CONTENTS

	<u>Page</u>
FORWARD	
ABSTRACT	
<u>SECTION</u>	
1. Introduction	1
2. Technical Discussion	5
2.1 Theory	5
2.1.1 Mathematical Models	5
2.1.1.1 The Collinearity Model	5
2.1.1.2 Gaussian Distortion	8
2.1.1.3 Decentering Distortion	8
2.1.1.4 Atmospheric Refraction	10
2.1.1.5 Film/Emulsion Deformation	11
2.1.2 Computational Problems	12
2.1.2.1 Instability of the Calibration Resection Computation	12
2.1.2.2 Update of Observables	14
2.2 Method of Mixed Ranges	16
3. Casa Grande/Mt. Graham MMR Experiment	21
3.1 General Description	21
3.1.1 The Casa Grande Range	21
3.1.2 The Mt. Graham Range	23
3.1.3 Casa Grande/Mt. Graham MMR Simulation	25
3.2 The Reconnaissance Survey	30
3.3 The Mt. Graham Geodetic Field Survey	35
3.3.1 The Horizontal Survey Results	37
3.3.2 The Vertical Survey Results	40
3.4 The Aerial Photography	42
3.5 Photo Coordinate Observations	44
3.6 The Adjustment	45
3.6.1 Preliminary Data Processing	45
3.6.1.1 Film Deformation	46
3.6.1.2 Parameter Approximations	47
3.6.2 Summary of Adjustment Results	47
3.6.2.1 Photo Coordinates	49
3.6.2.2 Comparison of Results	54
4. Conclusions and Recommendations	61
References	65
Appendix A	67
Appendix B	71

## 1. Introduction

The concept of calibration is formulated in the context of the measurement problem. If the goal is that of evaluating the performance of the objective lens of the aerial camera, then, the highly developed concept based on laboratory procedures serve well this purpose. These procedures assign numbers to principal point location, calibrated focal length, distortion, resolution, etc. of a specific objective lens. Such a concept of calibration is of great value to those concerned solely with optical design and performance. In contrast to this concept of calibration is that of measurement system calibration. It is this concept of system which is well developed by Eisenhart [1963] that is of paramount importance to the practicing photogrammetrist. Measurement system calibration requires first the definition of the total operational system followed by periodic evaluation of the operational system against a standard of comparison of higher accuracy. It is the product of such a system calibration that will ultimately serve to provide the photogrammetrist with means for improving his final product and for reliably estimating its accuracy.

With aerial photogrammetry, the system concept of calibration was for practical reasons set aside in favor of the immediately available laboratory calibrations. It is the author's opinion that it is this limited notion of calibration and the problems of adequate control of film shrinkage that have relegated aerial photogrammetry to a plateau of accuracy above which few expect it to rise.

With the introduction of reseau cameras, a significant improvement has resulted in film shrinkage correction. It remains to expand the calibration procedures into closer conformance to the concept of system calibration. The

problem that arises here is that of simultaneously determining certain highly correlated system parameters. The linear relationship in the conditional function between exposure station elevation and the camera constant over flat terrain is well known. Other unfavorable relationships exist as well. Schemes which conform to the system concept for the suppression of the high correlations have been suggested [Brown, 1969], [Moren, 1967], [Merchant, 1967, 1971]. In an outstanding experiment, Brown [1969] demonstrated a total and simultaneous treatment of the aerial photographic system under operational circumstances. Although too costly a procedure to recommend for routine and periodic sampling of system performance, it's singular results rising well above the contemporary accuracy plateau offers strong motivation for pursuing the development of realistic calibration of the aerial photographic system.

The Syracuse University Research Foundation received a contract from the Air Force Systems Command (RADC) in 1965 for the study of the problem of calibration of the aerial photographic system. One major result of this study was the preliminary findings in connection with three-dimensional targeted test fields for use in aerial photo system calibration [Merchant, 1967]. This work was expanded to look at alternative schemes under an RADC contract awarded in April, 1970 to The Ohio State University Research Foundation. As a result of this work, several calibration schemes were devised and reported upon [Merchant, 1971]. Guidelines for the study were primarily aimed at reducing the requirements for modification of the aircraft and eliminating the requirement for supporting equipment either on the ground or in the aircraft. As a result of this study there evolved the "Method of Mixed Ranges" (MMR) requiring only targeted ground stations. Absolutely no modification to the aerial system is required. Photography over a three-dimensional mountainous range is "mixed" with photography over a high density range such as Casa Grande by a least squares adjustment in which the elements of interior orientation are carried as common parameters to all exposures. Survey coordinates

of targets are carried also as additional parameters of the adjustment. This method of adjustment was suggested by Brown [1969]. Its application to a mountainous range is unique.

In the spring of 1971, a contract was again awarded The Ohio State University Research Foundation (Dept. of Geodetic Science) to undertake a limited demonstration of the MMR. This paper reports on the theory, procedures and results of this project.

The overall rms error of photocoordinates after adjustment was 5.1 micrometers. Significant improvement could be expected with some alterations to the Casa Grande Test Range targets for use with large scale photography.

The general conclusion is that the calibration of the aerial photographic system is feasible by the MMR. By repeated applications of the MMR, the concept of calibration according to Eisenhart could be fulfilled. The cost of photo system calibration can become competitive with conventional laboratory component calibration procedures.

The author is indebted to many for their contributions during the course of this project. The success of this project is in large part due to Mr. Sol Cushman for his work on the geodetic survey of Mt. Graham. Without his expert guidance, the duration of the field work would have been doubled with corresponding increase in closure errors. Thanks are due to Mr. Ray Lafferty for his enthusiasm and expert pilotage, and to Mr. K. Jeyapalan for his helpful discussions and management of the problems of data processing. Thanks are also due to Mr. George Leigh, Mr. H. Nagaraja and Miss Sandra Lewis for their good work in support of this project.

The outstanding cooperation of Rangers Sims and Burgess of the U. S. Forest Service at Safford, Arizona is gratefully acknowledged.

## 2. Technical Discussion

### 2.1 Theory

Modern computational photogrammetric procedures are generally based on the concept that the image forming ray passes from the object, through a point of exposure (the exposure station) to the image point; the three points lying on a common line. This concept is termed the "collinearity condition" and is normally imposed during the development of the general projective equations of photogrammetry rather than during the computational phase of the problem. This has been termed the "First Order Theory" [Bender, 1971]. "Second Order Theory" then accounts for the systematic departures from the first or idealized theory. Primary causes for departures in the aerial case are film shrinkage, atmospheric refraction and optical distortions arising from the lens and from disturbances to the atmosphere in the vicinity of the aircraft. The approach taken during this research was to adopt mathematical models to represent the first and second order theory. Aerial photography was then acquired over the several control ranges and a simultaneous adjustment was performed to determine estimates for those parameters of the mathematical models that define the system. In this way, the first phase of calibration, that of establishing the measurement specifications, can be realistically accomplished.

#### 2.1.1 Mathematical Models

##### 2.1.1.1 The Collinearity Model (General Projective Equations)

Assuming collinearity, the fundamental relationships between object space and image space coordinates may be termed the "General Projective Equations of Photogrammetry." Their derivations have been presented by many authors using various mathematics. However, the results are generally in the form presented here. In an earlier report, Merchant [1971] presented the development based on the assumption that the survey and photo coordinate systems are right handed. Rotations were all adopted as right handed with:

$\omega$  = primary rotation taken about an axis parallel to the survey X axis

$\varphi$  = secondary rotation taken about a once-rotated Y axis

$\kappa$  = tertiary rotation taken about a twice-rotated Z axis

The basic relationships between survey coordinates (X, Y, Z) and coordinates (X', Y', Z') in a system with an origin at the exposure station and with axes parallel to the photo are then:

$$(2.1) \quad \begin{bmatrix} X' \\ Y' \\ Z' \end{bmatrix} = \begin{matrix} M & M & M \\ \kappa & \varphi & \omega \end{matrix} \begin{bmatrix} X - X_0 \\ Y - Y_0 \\ Z - Z_0 \end{bmatrix}$$

where:

$M_{\kappa}, M_{\varphi}, M_{\omega}$  = rotation matrices corresponding to specific gimbal axis

$X_0, Y_0, Z_0$  = survey coordinates of the exposure station

At this point, the condition of collinearity is introduced thereby establishing similar triangles containing corresponding sides of the projections in the image and object space. Based on the assumption of collinearity, the relationships between corresponding sides of the resulting similar triangles are expressed as:

$$(2.2a) \quad \frac{x}{X'} = \frac{c}{Z'}$$

$$(2.2b) \quad \frac{y}{Y'} = \frac{c}{Z'}$$

or as:

$$(2.3a) \quad x = c \frac{X'}{Z'}$$

$$(2.3b) \quad y = c \frac{Y'}{Z'}$$

where:  $x, y, c$  = the photo coordinates of the image point  
 $X', Y', Z'$  = the photo parallel object space coordinates of the corresponding point

After substitution of equations 2.1 into 2.3 and then expanding, the general projective equations

(gimbal form) become:

$$(2.4a, 2.4b) \quad \left. \begin{aligned} f(x) &= (x-x_0) - c \left\{ \frac{(X-X_0) \cos \varphi \cos \omega + (Y-Y_0) (\cos \omega \sin \kappa + \sin \omega \sin \varphi \cos \kappa) + (Z-Z_0) (\sin \omega \sin \kappa - \cos \omega \sin \varphi \cos \kappa)}{(X-X_0) \sin \varphi - (Y-Y_0) \sin \omega \cos \varphi} + (Z-Z_0) \cos \omega \cos \varphi \right\} \\ f(y) &= (y-y_0) - c \left\{ \frac{-(X-X_0) \cos \varphi \sin \omega + (Y-Y_0) (\cos \omega \cos \kappa - \sin \omega \sin \kappa) + (Z-Z_0) (\sin \omega \cos \kappa + \cos \omega \sin \varphi \sin \kappa)}{(X-X_0) \sin \varphi - (Y-Y_0) \sin \omega \cos \varphi} + (Z-Z_0) \cos \omega \cos \varphi \right\} \end{aligned} \right\}$$

where:  $(x, y)$  = photo coordinates in a fiducial center system  
 $(x_0, y_0, c)$  = coordinates of the adopted "principal point" in the fiducial center system  
 $(X, Y, Z)$  = coordinates of the exposure station in the survey system  
 $(X, Y, Z)$  = coordinates of the object space point in the survey system  
 $(\kappa, \varphi, \omega)$  = gimbal angles defining the orientation between the survey and photo coordinate systems

NOTE: All coordinate systems are righthanded, all rotations are righthanded.  $(\omega)$  is primary,  $(\varphi)$  is secondary, and  $(\kappa)$  is tertiary when proceeding from the survey to the photo coordinate system.

### 2.1.1.2 Gaussian Distortion

Optical lens design based on Gaussian optics (First Order Theory) will result in disturbances to the image formation process even though the lens system may be perfectly centered and monochromatic light is employed. This approximation in design has been explored by Siedel and expressed in terms of five disturbances to image formation or the five Siedel aberrations. Of particular importance here is the distortion aberration. Professor A. E. Conrady (University of London) has demonstrated that the radial distortion aberration may be represented by an odd order polynomial in the radial distance ( $r$ ) from the optical axis. That is:

$$(2.5) \quad \delta r = K_1 r^3 + K_2 r^5 + K_3 r^7 - - - - -$$

A similar development with identical results has been used by Brown [1964]. Note that the distortion aberration may be characterized as being symmetrical about the optical axis, free of discontinuities, and non-existent on the optical axis. The radial symmetrical distortion may then readily be reduced to rectangular components in the photo plane resulting in:

$$(2.6a) \quad \begin{aligned} \delta x &= (K_1 r^2 + K_2 r^4 + K_3 r^6)(x) = K(x) \\ \delta y &= (K_1 r^2 + K_2 r^4 + K_3 r^6)(y) = K(y) \end{aligned}$$

### 2.1.1.3 Decentering Distortion

The practical inability for manufacturers to perfectly align the several optical axis of individual elements of a compound objective lens results in a series of aberrations similar to those described by Siedel but from a different source. Again, the aberration distortion is important in a metric calibration of the photographic system and will be termed "decentering distortion". The astronomers were concerned also with this problem and the ray tracing results of Conrady [1919] represented decentering distortion as follows:

$$(2.7a) \quad \delta r = 3P_3 v^2 \cos \chi$$

$$(2.7b) \quad \delta t = P_3 v^2 \cos \chi$$

where:

$\delta r, \delta t$  = radial and tangential components of distortion

$P_3$  = constant

$v$  = angle off the optical axis measured to the image point

$\chi$  = angle measured in the image plane from the axis of maximum radial distortion

The work of Conrady was adapted by Brown in a series of papers [Brown, 1964, 1965, 1966] which resulted in a model for decentering distortion in terms of rectangular coordinate components and in a form well suited for adjustment computations. The mathematical model to represent decentering distortions adopted for this research is that of Brown and is as follows:

$$(2.8a) \quad \delta x = [P_1(r^2 + 2x^2) + 2P_2xy][1 + P_3r^2 + \dots] = [Jx]$$

$$(2.8b) \quad \delta y = [2P_1xy + P_2(r^2 + 2y^2)][1 + P_3r^2 + \dots] = [Jy]$$

where:

$$P_1 = J1 \sin \varphi_0$$

$$P_2 = J1 \cos \varphi_0$$

$$P_3 = J2/J1$$

$$P_4 = J3/J1$$

$$P_5 = \dots$$

As noted by Brown [1965], in this model, the coefficients of  $P_1$  and  $P_2$  in the linearized form of the function can be adequately represented initially by assuming zero as a first approximation for  $P_3$ . As a consequence, first estimates taken as zero for parameters will not seriously influence convergence of the adjustment.

#### 2.1.1.4 Atmospheric Refraction

The aerial scene from conventional altitudes is particularly subject to the refraction of rays passing through the varying density levels of atmosphere from the ground to the exposure station. Studies have shown that for the extreme corner of the format ( $\alpha = 45^\circ$ ) and for the most extreme conditions of weather, the departure of a correction from that determined based on a generalized world wide, seasonably averaged model, is less than two micrometers for altitudes of approximately 15000 feet above sea level [Merchant, 1968].

For this research, the Air Research and Development Command (ARDC) 1959 Standard Model of the Atmosphere has been adopted. Based on the ARDC 1959 model, Dr. Bertram [ASP, 1966] proposed a model for aerial refraction representing the systematic affect on the imaging ray ( $\delta\alpha$ ) as:

$$(2.9) \quad \delta\alpha = R \tan \alpha$$

in which:

$$R = \left\{ \frac{2410 H}{H^2 - 6H + 250} - \frac{2410 h}{h^2 - 6h + 250} \frac{h}{H} \right\} \cdot 10^{-6}$$

where:

H = altitude of exposure station (km)

h = altitude of terrain point (km) taken  
generally as the scene average

#### 2.1.1.5 Film/Emulsion Deformation

Probably the most serious systematic departure of aerial photographic imagery from the idealized collinearity assumption is caused by the deformations experienced by the film (base/emulsion) combination between the time it is exposed and the time it or its next generation positive is measured.

Much information is available concerning the physical characteristics of the new stable base films [Kodak, 1965], [Brock, 1972]. Work has been reported concerning the interpretation of these physical characteristics into the environmental context of the aerial photographic mission [Merchant, 1968]. Analysis of actual data obtained from aerial photography subject to the normal extremes of mission environment have been reported [Brown, 1969], [Ziemann, 1968]. Some results of live data analysis regarding film shrinkage are presented in Section 3.7 of this report.

It appears that the consensus is that for consistently accurate correction to film distortions there is presently no equal to the methods which make use of a reseau. The reseau must be imaged simultaneously with the terrain features if it is to exert full effectiveness.

For this research, a Zeiss RMK-AR-15/23 precision camera was used. The optics are so designed that the last optical element possesses a second surface of infinite radius and lies from 40 to 60 micrometers from the photo emulsion plane. Upon this glass surface is recorded an array of crosses in the form of a one centimeter interval grid. This array of control (reseau) is projected the very short distance to the image at the instant of terrain exposure. The result is a dense array of imaged control by which film deformations and appropriate corrections can be determined on each photograph.

The reseau was used during this investigation for film distortion corrections. Each of the four reseau points bracketing the image of a ground target was observed once. Alternately, with each reseau point observation, an observation was made on the target image. The mean value of the target image

coordinates was transformed into the photo coordinate system by means of a general affine transformation. The six parameters of the transformation were determined separately for each target by a least squares adjustment of the eight observations provided through one pointing on each of the four bracketing reseau images. The mathematical model adopted for this transformation is then of the form:

$$(2.10a) \quad f(x) = 0 = x' - A_1 x - B_1 y - C_1$$

$$(2.10b) \quad f(y) = 0 = y' - A_2 x - B_2 y - C_2$$

The freedom of the general affine transformation accounts not only for the shift of origins, rotation of system axes, linear shrinkage along each axis independently, but also accommodates a component of film deformation which is non-orthogonal in character.

This is of course a rather conservative model in view of the fact that the complete control in all cases is within one centimeter of each target image. Alternative schemes for use of the reseau as shrinkage control which offer increased efficiency with moderate accuracy losses are presented by Ziemann [1968].

### 2.1.2 Computational Problems

The procedure for estimating the parameters describing the interior orientation of the camera and other parameters of the photo system is of course the method of least squares. The formulation of the observation equations and normal equations as used in this research was accomplished in detail and reported earlier [Merchant, 1971].

#### 2.1.2.1 Instability of the Calibration Resection Computation

The problems of instability in the computation arising from the geometry of the single photo resection in which both the elements of interior and exterior orientation are carried as unknown and unconstrained parameters have

been discussed earlier [Merchant, 1971]. If it can be demonstrated that one or more columns of the (B) matrix bear a scalar relationship to another column, the condition is described as linearly dependent. The consequence is that an infinite number of possible selections for the paired parameters exist; each of which will satisfy the observation equations with equal satisfaction. In other words, paired or higher combinations of parameters may not be separated by the adjustment when subject to such geometry. As examples, in the case of vertical photography over a level target field there is the influence of strict linear dependency existing between the following paired elements of interior and exterior orientation [Merchant, 1971]:

- a. principle point coordinate ( $x_0$ ) and exposure station coordinate ( $X_0$ )
- b. principle point coordinate ( $y_0$ ) and exposure station coordinate ( $Y_0$ )
- c. camera constant ( $c$ ) and the terrain clearance ( $H - h$ )

It is clear that computational problems will arise as calibration is attempted when such geometry is approached. For vertical photography, which is the conventional aerial case, there are basically two alternative approaches which have been suggested to suppress these unfavorable high correlations existing between interior and exterior elements of orientation.

The first is that suggested and employed by Brown [1969] for the analysis and calibration of the KC-6A cameras of the USQ-28 Geodetic Sub-System. In this approach, the exposure station coordinates were determined by means of three ground based stellar cameras occupying known survey stations and by using the star field for further control. These "observations" of the exposure station coordinates ( $X_0, Y_0, Z_0$ ) were introduced into the normal equations with appropriate weighting thereby altering the poorly conditioned normal coefficient matrix. The result was the strong separation of the interior and exterior positional parameters in the simultaneous adjustment computation.

The second approach makes use of a three-dimensional control range. An adaptation of this is the "Method of Mixed Ranges" (MMR) [Merchant, 1971]. It is the MMR which is used as the basis of this research.

#### 2.1.2.2 Update of Observables

In a recent paper, Pope [1972] points up problems that may be experienced in convergence of the non-linear least square problem when the solution of the normal equations is accomplished by the Newton-Gauss iterative method. According to Pope:

"If the expected values of all observables can be expressed as non-linear functions of parameters, then the least square adjustment by Newton-Gauss presents no problem."

It is of interest to relate this statement to the general form of the conditional functions of Brown for the case of direct observations of unknown parameters [Brown, 1969]. There are two forms of the conditional functions relating the observables to the unknown parameters. For observation of photo coordinates, the equations (2.4) in abbreviated form, including parameters of distortion are:

$$(2.11a) \quad x = x_0 + c \frac{\Delta X'}{\Delta Z'} (1 + K)^{-1} + [Jx]$$

$$(2.11b) \quad y = y_0 + c \frac{\Delta Y'}{\Delta Z'} (1 + K)^{-1} + [Jy]$$

Note that if only photo coordinates are observed, the observations  $(x, y)$  are non-linear functions of parameters only. The question of the existence of the radial distance term  $(r)$  implicitly in the  $(K)$  and  $(J)$  terms may cause concern. However, its influence on convergence is relegated to that of at least second order if  $(r)$  is defined in terms of the **image's distorted** coordinates. The choice of this function for relating observations of photo coordinates to the parameters is therefore appropriate, according to Pope, when only photo coordinates are observed.

The more general notion of Brown in which all parameters are taken also as observables raises a new question. For this case, a new form of the conditional function is formulated which relates the observables to the parameters [Brown, Davis, Johnson, 1964]. For direct observations of the elements of interior orientation, the chosen function is:

$$(2.12) \quad \begin{bmatrix} 1 \\ X \\ 0 \end{bmatrix} = \begin{bmatrix} 1 \\ X \\ a \end{bmatrix}$$

where:

$$\begin{bmatrix} 1 \\ X \\ 0 \end{bmatrix} = \text{the vector of directly observed elements of interior orientation}$$

$$\begin{bmatrix} 1 \\ X \\ a \end{bmatrix} = \text{the vector of adjusted elements of interior orientation}$$

In this procedure, the observables are again only functions of parameters; thus one avoids the "Pitfalls of Pope".

A similar case may be made for direct observations on the elements of exterior orientation and for survey coordinates of object space features.

In the adopted functions for treating observations of photo coordinates (equations 2.11), it is noted that the parameters are also observations and are in a non-linear function. However, since they are also treated as parameters, they are updated on each cycle of the iterative adjustment. Accordingly, both the parameters and the observables appearing as the independent variables of the non-linear functions (equations 2.11) are updated in each succeeding cycle of the Newton-Gauss iterative method of solution. Again, the "Pitfalls of Pope" have been avoided by updating of the observables in the procedures of Brown which have been adopted for this research.

## 2.2 Method of Mixed Ranges

The "Method of Mixed Ranges" (MMR) is an extension of the concept of three-dimensional control fields investigated by Merchant [1967] for the aerial case and by Torlegard [1967] for the close-range case.

It is convenient to discuss the basic distinctive geometric characteristic with reference to Table 2.1. This table indicates the ratio of coefficients for the indicated parameter pairs in the photo coordinate conditional functions (equation 2.4) for all observations of photo coordinates if the angular elements of exterior orientation are approximated as zero. It may be recalled from section (2.1.2.1) that the paired parameters cannot be separated in an adjustment based on a function in which the coefficients of one parameter in the set of all observations is a scalar multiple of a second parameter. That is, in Table 2.1, if the circumstances are such that any one of the terms in the "Ratio" column is a constant for all observations, these parameters cannot be separated and no unique solution in the usual sense is possible. Under the circumstances of a flat target field, provided no direct observations of parameters are introduced, it is evident that there are three parameter pairs that may not be separated within the described circumstances.

In the method employed to calibrate the KC-6A cameras [Brown, 1969], independent observations of  $(X_o, Y_o, Z_o)$  were introduced to destroy the singular characteristic of the normal coefficient matrix and permitted a solution for the corresponding interior elements.

For the MMR, an alternative approach is used. In Table 2.1, it can be seen that all coefficients are constant, provided the elevation,  $(Z)$  of all points remain constant. Conversely, the coefficients transform into variables as the elevation of points vary. Accordingly, the linear dependence in the conditional function for photo coordinates is destroyed and the corresponding parameter pairs may be separated in an adjustment in which there are no direct

Parameter Pair		Ratio of Coefficients #2 ÷ #1
#1	#2	
$x_o$	$X_o$	$-c/(Z - Z_o)$
$y_o$	$Y_o$	$-c/(Z - Z_o)$
$c$	$Z_o$	$c/(Z - Z_o)$

Table 2.1 Ratio of Coefficients of Selected Paired Parameters for the General Projective Equations Under the Assumption of Verticality (i.e.  $\kappa = \varphi = \omega = 0$ )

observations of exterior orientation elements.

The MMR exploits this characteristic of the three-dimensional control field. However, due to the need for a high density of imaged control to adequately determine parameters describing distortion, photography is also taken over a dense network of targeted control provided by existing control ranges. Photography over both the three-dimensional and flat target ranges are mixed in a simultaneous adjustment (thus, the method of mixed ranges) in which a common set of elements describing interior orientation for all photos is carried.

It is noted that the MMR requires no departure from operational circumstances; which is in accord with the concept of calibration according to Eisenhart. Note also that no modification to the aircraft is required or no external supporting equipment other than the targeted range is required. This is of great practical importance in procedures for calibration of existing aerial photographic systems.



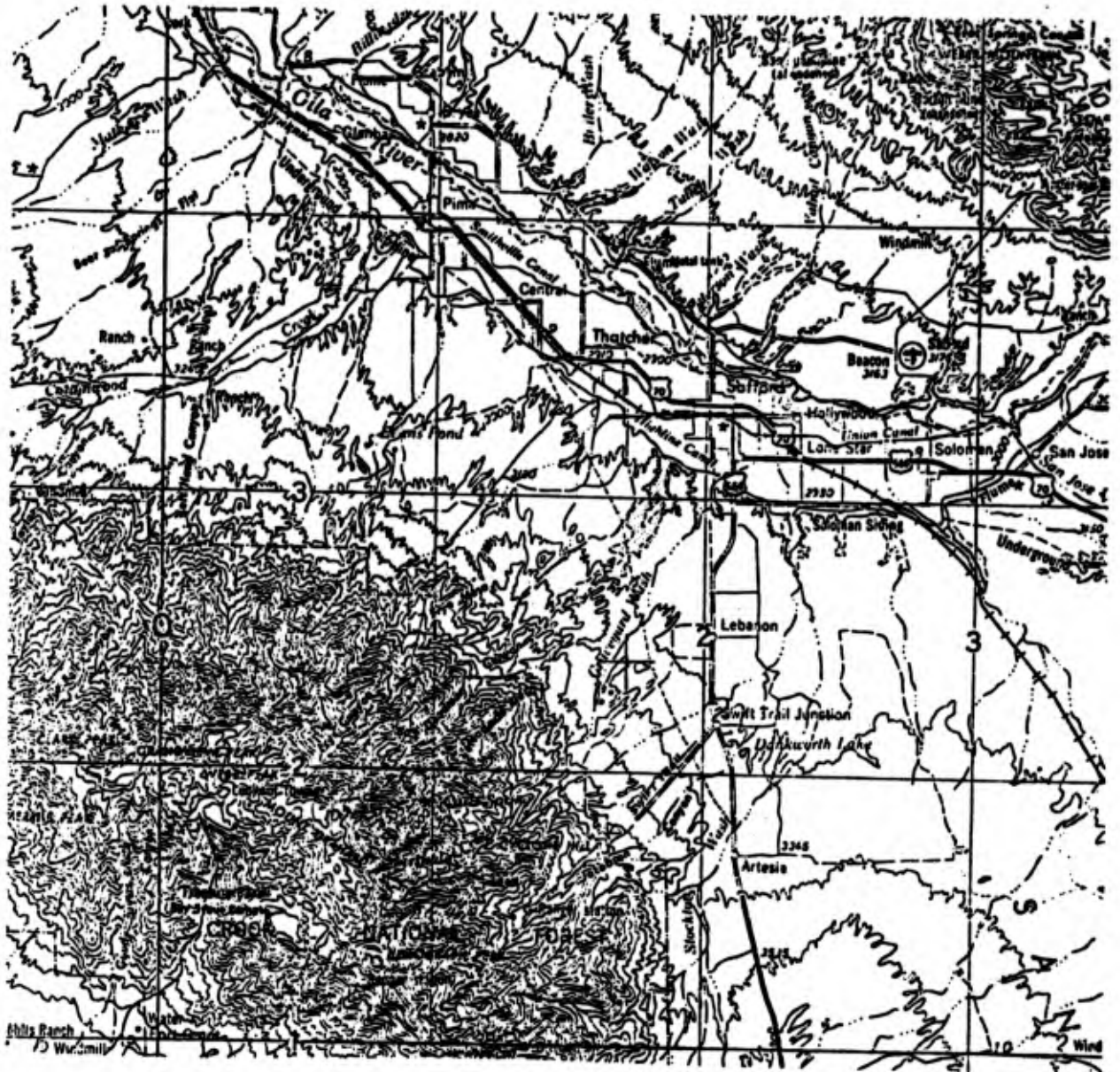


Figure 3.1b Mt. Graham Range (USGS, 1:250,000)

$\varphi = 32^{\circ} 38' N$  ,  $\lambda = 109^{\circ} 39' W$

Reproduced from  
best available copy.

### 3. Casa Grande/Mt. Graham MMR Experiment

#### 3.1 General Description

The purpose of this experiment with the MMR was to demonstrate the general feasibility of the procedures for dynamic aerial photo system calibration. A search was made to identify a site for the required three dimensional range. Factors bearing on the selection were:

- a. large height differences for points appearing in individual exposures
- b. proximity to an existing targeted calibration range (in this case, the Casa Grande, Arizona range)
- c. reasonable access by vehicle to facilitate the control survey
- d. distribution of existing geodetic control

After some compromise, a section of Mt. Graham in eastern Arizona was selected. Figures 3.1a and 3.1b indicate the locations and general relationships of the Casa Grande and Mt. Graham ranges.

##### 3.1.1 The Casa Grande Range

The Casa Grande Test Range is located in south central Arizona south of Phoenix. It consists of an array of targets approximately one mile on centers over an area approximately seventeen miles square. Figure 3.2 presents the details of the design of an individual target. Note that the design was guided by requirements for relatively small scale photography. Particular notice is directed to the ten foot open space defined by the inner edges of the wings of the cross. Because of the relatively large scale photography obtained for this investigation, it was the image of this relatively poorly defined void at the marker center which was observed on the photography. The consequences are discussed in Section 3.5.

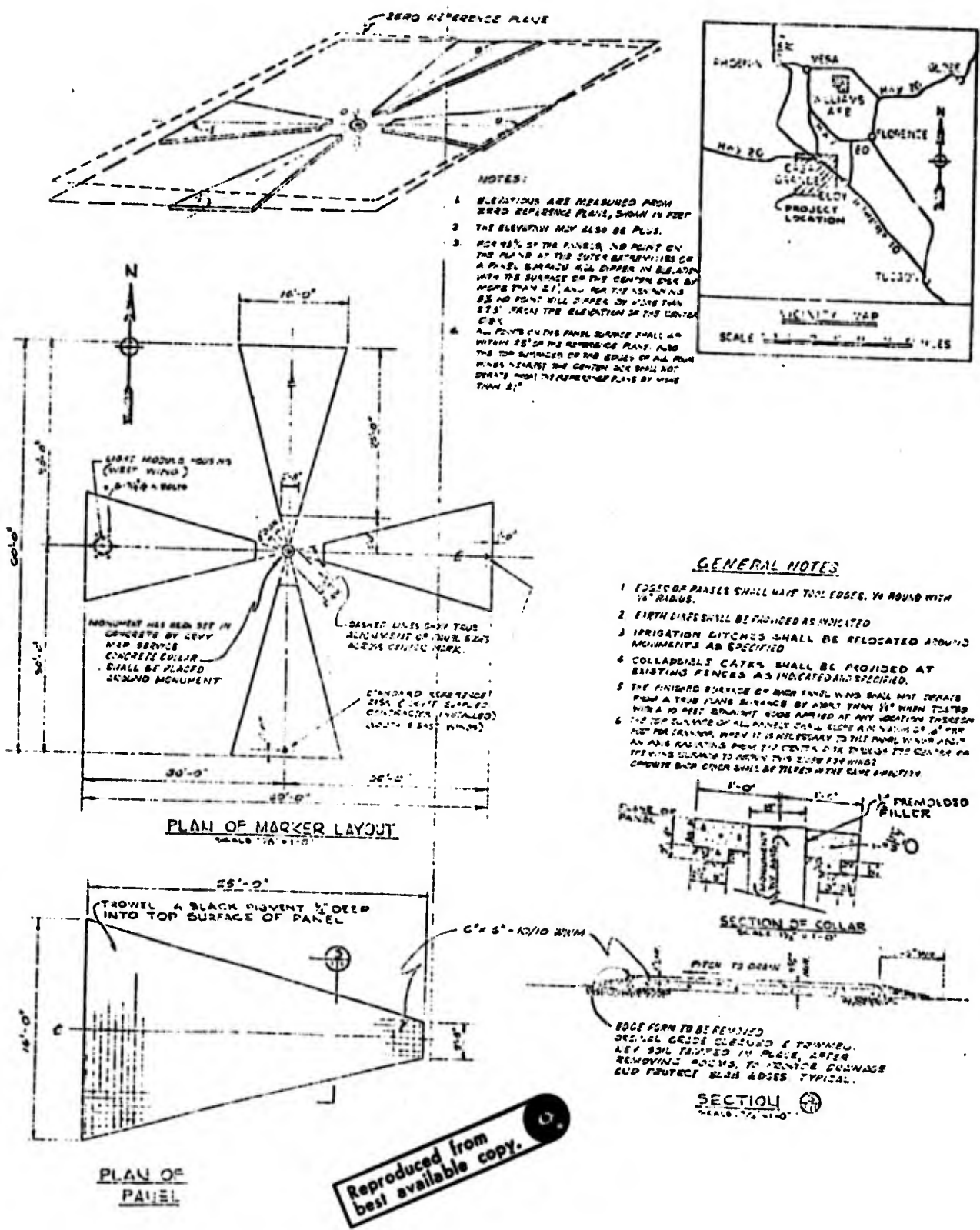


Figure 3.2 Target Detail, Casa Grande Range [USAE, 1968]

### 3.1.2 The Mt. Graham Range

The site selected for the three-dimensional range is located on the Swift Trail about twelve miles southwest of Safford, Arizona. The selection of stations was guided by an earlier analysis of geometry [Merchant, 1971]. The locations of the selected survey stations are indicated in Figure 3.3. Note the difference in locations of station (C') as determined from a study of the reconnaissance photography and the finally adopted location (C) after encountering virtually impossible terrain during the actual geodetic survey. As will be shown later by comparison of the synthetic and live data results, the reduction in height differences caused by the use of station (C) rather than (C') caused an increase in correlation between the camera calibrated focal length and the exposure station ( $Z_0$ ) coordinates.

The line between stations (D) and (A) is the longest of the survey (approximately 12,000 feet) and includes the points of greatest elevation differences within the Mt. Graham range (approximately 3000 feet).

Existing horizontal geodetic control within the chosen range was not considered to be of sufficient accuracy to be useful. However, a tie was made to station "Heliograph", USFS, 1934. Azimuth was obtained by Polaris observations. The adjusted horizontal values of the new geodetic survey are therefore in the national network (NAD 1927).

The vertical control was for the most part destroyed due in large measure to the continuous road maintenance program. All vertical control for the new survey was based on a single undisturbed bench mark located in the vicinity of station (A). The bench mark (GAR W BM NO 7, Elev. 603, 1934) elevation had been determined by less than third order methods and is published to the nearest foot only. (Sea Level Datum, 1929)

In summary, existing geodetic control was of no value other than permitting the adjusted horizontal values of the Mt. Graham range to be computed nominally in terms of the national network. The internal accuracies to be

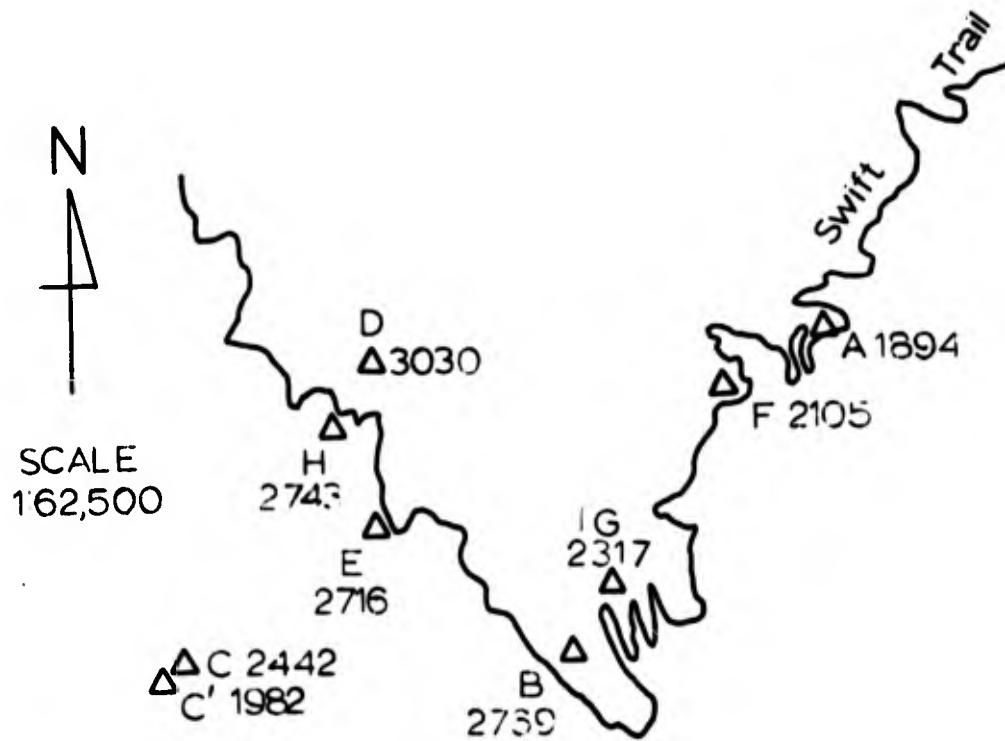


Figure 3.3 Target Locations, Mt. Graham Range (elevations in meters)

discussed later are on the order of one part in 50,000 closures in the horizontal and 0.04 meters closure in the vertical.

### 3.1.3 Casa Grande/Mt. Graham MMR Simulation

After the selection of Mt. Graham as the site for the required three dimensional range, an investigation was initiated to offer assurance that the geometry of Mt. Graham would be adequate. The study considered not only the geometry of the range/camera/exposure combinations but considered also the influence of realistic errors associated with all observations.

The basic tool required for this study is the digital computer. For this purpose and for subsequent use, the program entitled CALIB was developed after the method of Brown. The mathematical models were those described in Section 2.1.1. The adjustment was by the method of least squares. The notion that all parameters were also "directly" observed quantities was used.

The synthetic data consisted of the true values of survey coordinates  $(X, Y, Z)$ , elements of exterior orientation  $(\kappa, \varphi, \omega, X_o, Y_o, Z_o)$ , the limited set of elements describing interior orientation  $(x_o, y_o, c)$  and the corresponding photo coordinates  $(x, y)$ . This was accomplished for each of twelve exposures; four in the cardinal directions over Mt. Graham and eight over Casa Grande. The unaltered general projective equations, gimbal form, were used (equations #2.4). Note that no parameters were introduced in the synthetic data distortion for the simulation. It was felt that the primary purpose was to demonstrate an acceptable level of separation of the paired positional parameters between interior and exterior orientation (see Section 2.2). Other correlational problems were not assumed to be strongly sensitive to the geometry of the three-dimensional range. However, distortion parameters were carried as unconstrained parameters in the adjustment. The influences of correlations and observational residuals in generating values for terms ex-

pressing distortion (which in fact did not exist) in the unperturbed data is evidenced by the numerical values computed for the models of distortion. However, an alteration to the computed focal length of only  $-6\mu\text{m}$  will cause the distortions to be essentially non-existent.

Table 3.1 indicates the values selected for introducing normally distributed perturbations to the true values of the parameters. The mean of the distribution was taken as zero in each case.

The selection of target locations in the several ranges was based on the demonstrated absolute ceiling of the aircraft as well as on the topography of Mt. Graham and the existing locations of targets on the Casa Grande range. These adopted target locations are indicated in Figure 3.4.

The resulting location of the sum of all target images is indicated in Figure 3.5. This target image distribution serves to point out the problem of imaging a uniform array of targets such as provided by the Casa Grande range on photography taken from a limited altitude. Selection of photography should be based on obtaining the maximum density of targeted images and on obtaining a random distribution within the format. The reasoning here is that the higher density will assure a "better" estimate of the parameter values and that the random character of the target images will reduce the possibility of neglecting significant cyclic trends in the data. In the case at hand, the absolute ceiling of the aircraft was taken as about 17,000 feet for the seasonal conditions at Casa Grande. This meant, that with some good fortune, a single photo could be expected to just image five rows and five columns of targets spaced uniformly at one mile intervals. The conflict arose then in selecting exposures in which all twenty five targets were imaged but with almost identical format locations for all exposures or selecting exposures which could provide a better target image distribution but at the expense of losing from five to nine target images (out of a possible twenty five). This of course would not be a severe problem if a

Parameter	$\sigma$	Parameter Description
$x, y$	5 micrometers	photo coordinates
$x_0, y_0, c$	50 micrometers	principal point coordinates and camera constant
$X_0, Y_0, Z_0$	2 meters	positional elements of exterior orientation
$\kappa, \varphi, \omega$	5 degrees	rotational elements of exterior orientation
$X, Y$	0.05 meters	horizontal survey coordinates
$Z$	0.08 meters	vertical survey coordinates

Table 3.1 Standard Deviations Assigned for Purposes of Parameter Perturbation During Generation of Synthetic Data.

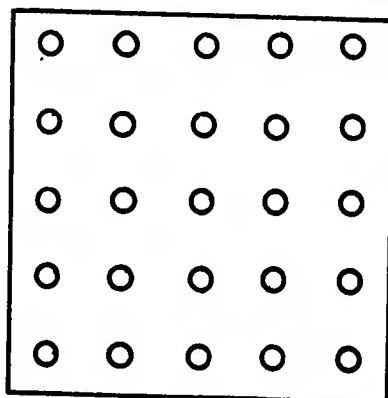
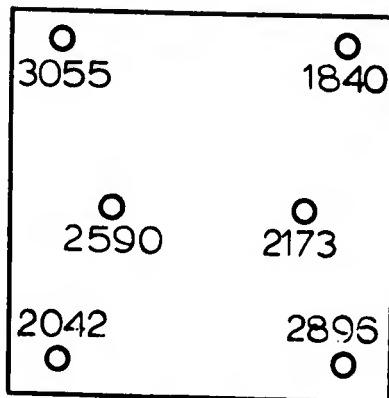
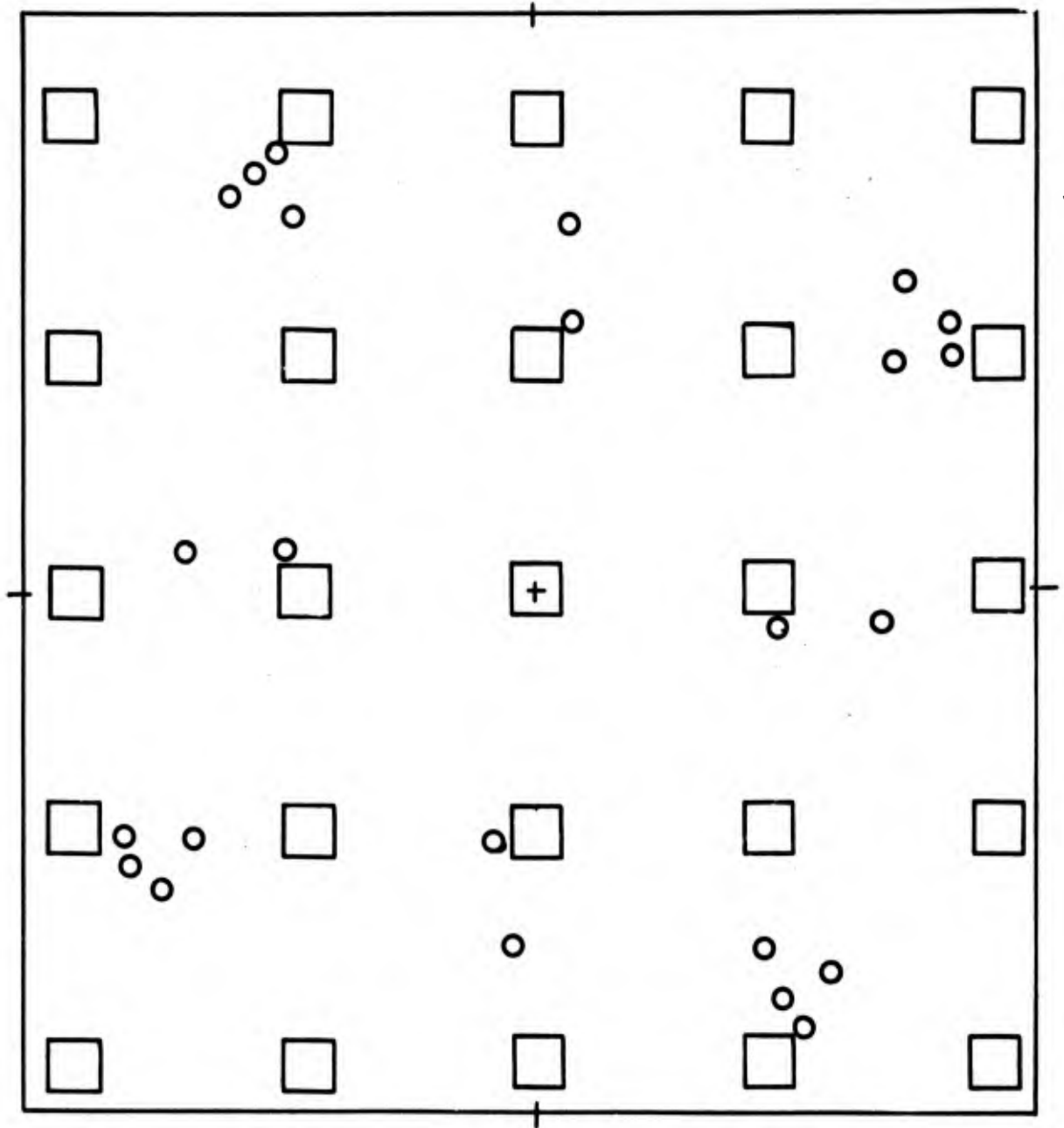


Figure 3.4 Range Target Locations for Synthetic Data Experiment [Jeyapalan, 1972]



○ - Mountain range target image locations

□ - Level range target image groupings (6 targets each)

Figure 3.5 Combined Image Locations of Targets for the Twelve Photos of the Synthetic Data Experiment

more dense array of targets were available or an aircraft capable of higher altitudes were employed over the Casa Grande range.

The adjustment simulation was conducted with the sum of target images as indicated in Figure 3.5. The results of the adjustment are presented in Table 3.2 and 3.3. Table 3.4 indicates the correlation coefficients relating parameters representing distortion, positional interior, and positional exterior orientation elements. Note that a distinction is made between exterior positional parameters over Mt. Graham with those from exposures made over Casa Grande.

These results indicated that the Casa Grande/Mt. Graham ranges together with observations approximating the accuracies chosen for this simulation would provide adequate parameter estimation and separation for purposes of demonstrating feasibility of the MMR approach to aerial photographic system calibration. The false indication of distortion emphasizes the danger in attempting to ascribe physical significance to individual parameters after adjustment when high correlation exists. The increase in strength of such parameter separation is the basic problem faced with this dynamic calibration procedure. However, even the correlation values of (0.90) and (0.95) between the camera constant and the flight height (Table 3.4) still appear to yield acceptable positional values as evidenced by the comparison of "true" and "computed" parameter values in Tables 3.2 and 3.3.

### 3.2 The Reconnaissance Survey

After the selection of Mt. Graham as the site for the three-dimensional target range, an aerial and ground reconnaissance was conducted.

An aerial survey was made using a Cessna 195 equipped with the Zeiss RMK-AR camera. Overflights were made of both the Casa Grande and Mt. Graham ranges at the aircraft's absolute ceiling and considerable photography was obtained. Using the target image from the Casa Grande range as control, a

Mountainous Terrain Exterior Orientation Elements (Mt. Graham)

	Meters			Radians			Maximum Photo Coordinate Residual Micrometers
	X <sub>0</sub>	Y <sub>0</sub>	Z <sub>0</sub>	κ	φ	ω	
Computed Parameter	10975.18	8749.61	5241.58	0.000011	0.000081	0.00012	4
True Parameter	10975.0	8750.0	5242.0	0.0	0.0	0.0	
Apriori Weights	0.0	0.0	0.0	0.0	0.0	0.0	
Apostriori Std.Dev.	+0.3	+0.4	+0.3	+0.00002	+0.00009	+0.0001	

Level Terrain Exterior Orientation Elements (Casa Grande)

Computed Parameter	4299.93	4300.17	5241.22	0.000002	0.000012	-0.000027	5
True Parameter	4300.00	4300.00	5242.0	0.0	0.0	0.0	
Apriori Weights	0.0	0.0	0.0	0.0	0.0	0.0	
Apostriori Std.Dev.	+0.2	+0.2	+0.6	+0.000006	+0.00002	+0.00002	

Table 3.2 Representative Results for Exterior Orientation for an Adjustment Based on a Simulation of Twelve Exposures (MNR)

	$x_0(\mu)$	$y_0(\mu)$	$f(\text{mm})$	$K_1 \times 10^{-7}$	$K_2 \times 10^{-11}$	$K_3 \times 10^{-16}$	$P_1 \times 10^{-7}$	$P_2 \times 10^{-7}$	$P_3 \times 10^{-18}$
Computed Parameter	-7.0	3.0	149.981	0.14	0.14	0.4	0.2	0.7	0.0
True Parameter	0.0	0.0	150.000	0.0	0.0	0.0	0.0	0.0	0.0
Apriori Weights	0.0	0.0	0.0	0.0	0.0	0.0	0.0	0.0	100.0
Apostriori Std. Dev.	+6.0	+6.0	+0.018						

Variance of Unit Weight = 1.2

Table 3.3 A Comparison of Results for Interior Orientation After Adjustment Based on a Simulation of Twelve Exposures (MMR)

	Mt. Graham					Casa Grande						
	$K_1$	$K_2$	$K_3$	$X_0$	$Y_0$	$Z_0$	$\nu_j$	$Y_0$	$Z_0$	$P_1$	$P_2$	$P_3$
$x_0$	-	-	-	0.2	-	-	0.8	-	-	-0.2	-	-
$y_0$	-	-	-	-	0.2	-	-	0.8	-	-	-0.3	Constrained
$f$	-0.3	0.2	-0.2	-	-	0.90	-	-	0.95	-	-	-

Table 3.4 Correlation Coefficients After Adjustment Based on a Simulation of Twelve Exposures (MMR)

series of photogrammetric resection computations indicated that the maximum geometric altitude that was attained was on the average 16,850 feet above sea level. If the average terrain elevation of the Casa Grande range is taken as 1,450 feet, the terrain clearance is then 15,400 feet. On this basis, the single photo ground coverage exceeds by 10 per cent that required to image a 5 x 5 array of targets over Casa Grande. The significance of this limited altitude, directly restricting the distribution of target images, has been discussed in Section 3.1.3. Actual imagery verified this result with target images clustering into close patterns at twenty five format locations.

The same altitude restriction pertained to the Mt. Graham reconnaissance photography. As a result, the areas for selection for the low terrain points were moved up the S.W. and N.E. faces of Mt. Graham. Based on a study of the Mt. Graham photography, the areas for location of the two low targets were at 6100 feet and 6000 feet above sea level and the high target areas were at 10,000 feet and 9300 feet above sea level. Using the average values, the difference in elevation afforded in a single exposure by the geometry of Mt. Graham was 3600 feet. Using the absolute ceiling of 16,850 feet, the ratio of terrain elevation difference to exposure station elevation above the low targets became (0.34) or 34 per cent.

The aerial reconnaissance survey was of great value for determining realistic values for the simulation described in Section 3.1.3. In addition, a firm choice of target location areas could be made. The open regions suitable for targets on the high and low sections of the range which could be covered by a single exposure were clearly identified. Subsequent use of the photos during the geodetic field work proved to be of great value for planning access to the more remote stations. Estimated locations of open lines of sight between stations were also obtained from the reconnaissance photography.

The ground reconnaissance consisted of recovery of existing geodetic control and initial planning of the survey. The target areas were each visited (with the exception of Station C) and lines of sight tentatively verified. During this phase of the survey it was planned to use the fire watch tower at station "Heliograph" for an observation station. Subsequently, during the actual survey, this station was abandoned in favor of a more stable ground station at some loss in visibility. Detailed descriptions and ties for each station are presented in Appendix B.

The results of this phase of the reconnaissance indicated that the geodetic field survey would be conducted in a region within which few resources would be available other than what could be hauled in. In brief, only fresh water was available. There was no power, no fuel, no communications, no supplies nor accommodations. The only connection with the outside world was by a 25 mile unpaved mountain road. Preparations for the geodetic field survey were made accordingly.

### 3.3 The Mt. Graham Geodetic Field Survey

The primary stations established by geodetic survey on Mt. Graham for purposes of this research are indicated in Figure 3.2. All line lengths and all horizontal angles were observed between these stations or their immediate eccentrics. These observations were all conducted after dark for better conditions of atmospheric stability.

All horizontal angles were observed in at least four plate positions by using the Wild T-3 theodolite. The plate bubble was observed on each pointing and subsequently mis-levelment corrections were computed and applied. This was particularly critical for mountain type surveys as evidenced by the form of the correction formula:

(3.1)

$$\delta\alpha = z \tan \beta$$

where:

$\delta\alpha$  = correction to observed direction due to inclination  
( $\iota$ ) of the instrumental vertical axis

$\iota$  = inclination of instrumental axis from local survey  
vertical axis

$\beta$  = elevation angle of the line of sight taken as zero  
at the horizon

For surveys conducted in level regions, ( $\beta$ ) is small and the correction for small values of ( $\iota$ ) is second order in affect. Not so in mountainous work in which, in this case for example, ( $\beta$ ) was approximately 17 degrees from stations (A) to (D).

The slant range distances between stations as indicated in Figure 3.2 were observed at night by means of an AGA Geodimeter Model 6. Care was taken to calibrate and align the instrument prior to this survey. No difficulties were experienced in the use of this instrument.

The elevation differences between the primary stations of the survey were determined by a method of simultaneous reciprocal trigonometric leveling. Vertical angles were observed simultaneously from both ends of a line by using the objective lens of the alternate T-3 as a target. For the longer lines, special targets were constructed. The observations were coordinated by radio to assure that the data gathered at each station was essentially simultaneous, thus subject to the same anomalous atmospheric conditions. Vertical positions were observed until the last three positions did not exhibit a spread exceeding ten arc seconds at both ends of the line. This observational procedure was repeated at 10:00 a.m., noon, and 2:00 p.m. for each line of the survey. Daytime observations were used for vertical work to provide maximum mixing of the atmosphere thereby avoiding the possibility of including fixed anomalous refraction conditions. The mean values of these observations along with theodolite and signal heights were used to

compute station elevations according to standard U.S. practice.

### 3.3.1 The Horizontal Survey Results

The field work data was reduced and checked for inconsistencies. Individual loop closures were computed in the field. These closure errors are indicated in Table 3.5.

Loop (Refer to Figure 3.2)	Closures (meters)	
	X	Y
D - A - B - D	-0.028	-0.010
D - Fe - B - D	-0.102	+0.050
D - G - Be - D	-0.025	+0.003
D - E - H - C - B - D	+0.006	+0.096

Table 3.5 Individual Horizontal Loop Closures Before Adjustment for the Mt. Graham Survey

The closures were quite acceptable and the remaining field work for the horizontal survey consisted of preparing the station descriptions (see appendix B) and abstracting the observations.

The preparations for the horizontal survey adjustment were made by computing approximate geodetic coordinates for all stations. These computations were based on a tie to station Heliograph, 1934 (USFS) and an observational set on Polaris for scheme azimuth. The adjustment for the first three loops indicated in Table 3.5 was conducted simultaneously by least squares. Weights on distances were based on a standard error of 2 centimeters and directions on 2 arc seconds. The last loop was adjusted independently by traverse methods by holding stations (B) and (D) as fixed from the previous adjustment. The values finally adopted after adjustment for horizontal geodetic coordinates are indicated in Table 3.6. Based on the adjusted coordinates, the

STATION NAME	LATITUDE	LONGITUDE
A	32 38 59.80877	109 48 29.77518
F	32 38 39.57501	109 48 57.17638
G	32 37 46.52178	109 49 12.33060
B	32 37 35.98639	109 49 51.27152
E	32 38 7.55703	109 50 50.09379
H	32 38 42.50232	109 51 14.24307
C	32 37 46.41240	109 51 17.09997
D	32 38 54.22000	109 50 54.13000

Table 3.6 List of Adjusted Geodetic Coordinates for the Mt. Graham Survey (Tie to USFS Heliograph, 1934 and orientation by observation of Polaris yields nominal coordinates in the national system, NAD 1927)

FINAL INVERSES

FROM	TO	FORWARD AZIMUTH	BACK AZIMUTH	DISTANCE (meters)
A	B	39 26 58.47787	219 26 14.52413	3343.558
A	D	87 23 26.86164	267 22 8.98314	3766.118
B	D	145 47 38.40308	325 47 4.50209	2914.127
B	C	98 10 30.25570	278 9 43.97837	2260.322
E	D	175 48 51.94925	355 48 49.77217	1441.254
E	H	149 41 7.77233	329 40 54.74710	1246.579
F	B	35 45 9.07847	215 44 39.90536	2413.518
F	D	98 25 38.73594	278 24 35.64504	3081.348
G	B	72 16 25.99059	252 16 4.99426	1065.732
G	D	128 10 20.58095	308 9 25.67606	3374.810
H	C	2 28 5.09052	182 28 3.54974	1729.400

Table 3.7 List of Final Values of Azimuth and Spheroidal Distances for the Mt. Graham Survey

final values for forward and back azimuths and spheroidal distances were computed by an inverse computation and are presented in Table 3.7.

The estimated relative internal standard error was approximately one part in 50,000 with respect to the center of the survey.

### 3.3.2 The Vertical Survey Results

The field reduction of observations was rechecked and final mean observations compiled. An initial elevation above the sea level datum was obtained to the nearest foot by means of a differential level line from the only known existing bench mark (GAR W BM NO. 7, Elev. 603, 1934) to station (A). Holding the elevation of station (A) and using the observed differences in elevations between stations of the survey, the loop elevation closures were computed and are presented in Table 3.8. The closures appeared to be quite acceptable.

Loop (Reference to Figure 3.2)	Elev. Closures (meters)
D - A - B - D	-0.052
D - Fe - B - D	+0.040
D - G - Be - B - D	+0.023
D - E - H - C - B - D	+0.060

Table 3.8 Individual Vertical Loop Closures Before Adjustment for the Mt. Graham Survey

The least square procedure was used by employing the method of "observation equations." The initial approximate elevations, the station alterations, and the finally adopted station elevations are presented in Table 3.9.

Station	Approximate Values (meters)	Correction (cms)	Adjusted Values (m)
A	1894.27	-0.8	1894.26
B	2769.03	-2.0	2769.01
C	2442.21	-3.1	2442.18
D	3030.30	-1.2	3030.29
E	2716.37	-5.1	2716.32
F	2104.88	-2.7	2104.85
G	2316.91	-2.0	2316.89
H	2742.76	-3.9	2742.72

Variance of unit weight = 0.45  
Degrees of freedom = 3

Table 3.9 Results of Internal Adjustment of Elevation Differences for the Mt. Graham Survey [Jeyapalan, 1972].

### 3.4 The Aerial Photography

The photography over both the Mt. Graham and Casa Grande ranges was obtained during the morning of July 26, 1971.

The flight left the Safford, Arizona airport at 7:30 A.M. with R. Lafferty as pilot and D. Merchant as photographer. The goal was to obtain the photography prior to the development of "perch" clouds over the mountains which usually occur by 11:00 A.M. It was understood that the development of perch clouds is characteristic of the summer season in Arizona. The early start was to assure that the maximum altitude could be obtained well prior to the cloud development. The slow spiraling climb permitted close visual examination of all targets on the mountain range.

The maximum altitude of about 17,000 feet (a.s.l.) was obtained by 9:00 A.M.. Test passes were made over the range in the four cardinal directions. An identifiable feature was selected at the center of the range on the ridge midway between stations (B) and (D). The test passes permitted the drift to be established both for purposes of swing angle setting of the camera and for assurance that the center of the range would be included in the flight track. The proper setting of the camera swing angle was important to assure that target images would appear as nearly as possible in the extreme corners of the photo format.

The Zeiss RMK-AR camera occupied a heated but unpressurized compartment within the aircraft. No photographic window was used. The camera and filter combination were simply placed in the open well in the fuselage at about the center of lift of the Cessna.

The exposure data used throughout were:

aperature = f/8  
shutter = 1/300 second  
filter = type B ("minus blue")  
film = Kodak type 2402 (Plus-X)

Live photo passes began about 9:30 A.M. and continued until about 10:00 A.M. at which time the cloud formations began to cross the range.

Holding the altitude, the course was set for Casa Grande, 100 miles to the west. Upon arriving at Casa Grande the visibility was excellent and no cloud problem existed. A target region immediately to the south of the city of Casa Grande was selected and repeated test and live photo runs were conducted. Attempts were made to cover the same targets thereby reducing the number of survey coordinates required to be carried as parameters in the adjustment.

By 11:30 A.M., the last of the film was used. The fuel was approaching a similar condition. The photo mission was concluded at 11:45 after requesting a straight in approach at Coolidge-Florence Municipal airport a few miles east of Casa Grande.

During live photo runs, care was taken to initially expend approximately ten frames to assure uniformity of shrinkage and normal camera operation. The unavoidable nose high attitude of the aircraft exceeded the level limits of the camera mount by several degrees. However, no vignetting nor excessive vibrations appear to have resulted from this circumstance.

After refueling, the exposed film was flown to Tucson, Arizona for processing. The processing was accomplished by Cooper Aerial Surveys.

The film was developed in a rewind type continuous roll processor (Morse M-10) unit using Kodak - "HC110" (high concentrate) developer. The development continued for 21 minutes at a temperature of  $69\frac{1}{2}$  degrees F. A stop with hardener was used followed by ten minutes in Kodak-"Rapid Fix" fixer. The film was then washed and treated with Kodak-"Photo Flo". Drying was accomplished on a forced air continuous dryer (Type A-10). A preliminary review of the film indicated satisfactory development and contrast. A review of target images from the Mt. Graham photography indicated that at least six acceptable photos had been obtained. The Casa Grande photography included

a great number of useful frames and was also judged to be of satisfactory quality. A detailed description of the Zeiss RMK-AR camera used for this work is presented in Appendix A.

### 3.5 Photo Coordinate Observations

The photo coordinate observations were made on the Zeiss PSK stereo-comparator located at the Department of Geodetic Science. Some difficulties were experienced in the analog to digital encoders on this comparator. Consequently, one of the ten photos used for this work was measured on the department's P-CAT comparator. The calibration for both comparators has been established and the accuracy of both comparators is estimated to be better than two micrometers.

The images observed were of three types. Images were produced from reseau crosses, circular targets on the Mt. Graham and cross targets on the Casa Grande ranges.

The reseau image is produced by the projection of an opaque cross having a bar width of about 15 micrometers. The projection is from the second surface of the last element of the lens for a distance of about 40 micrometers. The result is a crisp image. The typical standard error of one observation on the reseau image is less than two micrometers. Some variation can be experienced due probably to variations in diapositive plate production.

The images produced on Mt. Graham photography were from circular flat white targets on flat black backgrounds. The diameters of the white circular targets were chosen such that the images would have nominal diameters of 50 micrometers. For example, the diameter of the target at station (D) at an elevation of 10,000 feet was 2.3 feet. The target diameter at station (A) at an elevation of 6200 feet was 3.9 feet. The quality of these images appeared to be quite good. The observational procedure called for a pointing on the target image after each pointing on the four bracketing reseau images.

The analysis of all observations indicated that the standard error of one observation on an image of a Mt. Graham target (pooled for x and y) was 2.7 micrometers. The mean value of four observations on an individual target image was used as the observed quantity in the calibration adjustment.

The images of targets on the Casa Grande photography were somewhat less satisfactory. The Casa Grande targets are crosses with tapered wings converging to the center but truncated to leave a ten-foot square opening directly over the station. The targets were constructed of concrete but treated to produce a dark flat finish. The finish contrasted with the natural light color of the bare soil in this region. Such a target design, although quite acceptable for much smaller scale imagery, left only the void at the center of the target image as the mark. The analysis of all Casa Grande photography indicated that the standard error of one observation was 6.7 micrometers. Even at the 99 per cent confidence level, the hypothesis that these observations have been drawn from the same population must be rejected.

Recommendations for improving the Casa Grande range for use on larger scale imagery will be made.

### 3.6 The Adjustment

The adjustment of all observations was conducted simultaneously by the method of least squares. Six photographs of the Casa Grande and four of the Mt. Graham ranges were mixed in the adjustment by carrying the elements of interior orientation as common parameters for all exposures. Other parameters were the unconstrained elements of exterior orientation for each of the ten exposures and the constrained survey coordinates for all targeted points.

The details of the adjustment method have been described earlier, [Merchant, 1971].

#### 3.6.1 Preliminary Data Processing

The comparator coordinates of target images were processed by computer to correct for atmospheric refractions and film deformation effects. The

model adopted for atmospheric refraction was presented and discussed in Section 2.1.1.4. The model for film shrinkage, discussed in Section 2.1.1.5 was based on a two dimensional general affine transformation. No corrections were applied for lens distortion in that these disturbances to the collinearity model were to be determined by the adjustment in terms of assigned values to distortion model parameters.

### 3.6.1.1 Film Deformation

As described earlier, the comparator coordinates on each target image on each photo were transformed into the reseau coordinate system by using observations on the four bracketing reseau images. The affine model possessed six parameters; thus, a modest over determination of the parameters was available at each target image. The unit standard error was computed after adjustment at each point and for each photo. The unit standard error provided an indication of the fit of the adopted transformation to the observed comparator coordinates. These values were averaged separately for the two targeted ranges and are presented in Table 3.10.

Range	Unit Standard Errors (Micrometers)	Number of Observed Targets
Casa Grande	2.8	97
Mt. Graham	2.6	28

Table 3.10 Unit Standard Errors After Transformation for Film Deformation Correction (affine transformation on four bracketing reseau point images)

There is evidently good agreement of the affine model to the observed reseau coordinates as well as good agreement between results from both ranges.

There is quite an interesting agreement between this result and that of Brown [1969] for the fit of the model to the reseau point image. In

the present experiment a general affine transformation (6 parameters) employing the images of the four bracketing reseau points was used with an average fit of 2.7 micrometers. Brown used a 16 parameter model to fit 37 reseau point images over the entire format. The average fit in that case was 2.6 micrometers. Some improvement in Brown's fit was experienced by dropping those reseau images at the film edges during the adjustment. In this way, the film region of susceptibility to non-uniform temperature and humidity conditioning was avoided.

#### 3.6.1.2 Parameter Approximations

The use of non-linear conditional functions led to an approximation by Taylor's series which requires estimates of values for the unknown parameters for its evaluation. For this purpose, the photography over Casa Grande and over Mt. Graham were treated separately in a simultaneous block adjustment. This served two purposes. The values computed for exterior orientations and for survey coordinates provided good first approximations to the parameters for use in the adjustment for calibration. Secondly, blunderous data could to some extent be detected and replaced or omitted. It was the problem of blunder detection that occupied a large amount of time during this investigation and will deserve special attention in future work.

#### 3.6.2 Summary of Adjustment Results

A broad summary of the characteristics of the Mt. Graham/Casa Grande calibration adjustment pertaining to the Zeiss RMK-AR 15/23 camera (Serial No. 21-197) are presented in Table 3.11. The parameters of the adjustment and their apriori weights are indicated in Table 3.12.

Due to the need for locating target images in the extreme corners of the format for photography of Mt. Graham and due to the problems in navigating a light aircraft at its maximum ceiling, a great number of exposures were taken in each of the cardinal directions. The hope was to chose one frame

No. of Photographs	10
Casa Grande	6
Mt. Graham	4
No. of Control Points	58
Degrees of Freedom	206
Variance of Unit Weight	1.73
No. of Iterative Cycles	3

Table 3.11 Summary of Characteristics of the Mt. Graham/Casa Grande Adjustment for Calibration

Parameters	Assigned Weights	Aprori Estimates of Standard Errors
$c, x_0, y_0$	0	-----
$K1, K2, K3$	0	-----
$P1, P2$	0	-----
$x, y$	40,000	0.005 millimeters
$X_0, Y_0, Z_0$	0	-----
$\kappa, \varphi, \omega$	0	-----
$X, Y$	400	0.05 meters
$Z$	150	0.08 meters

Table 3.12 Parameters of the Calibration Adjustment and their Assigned Weights

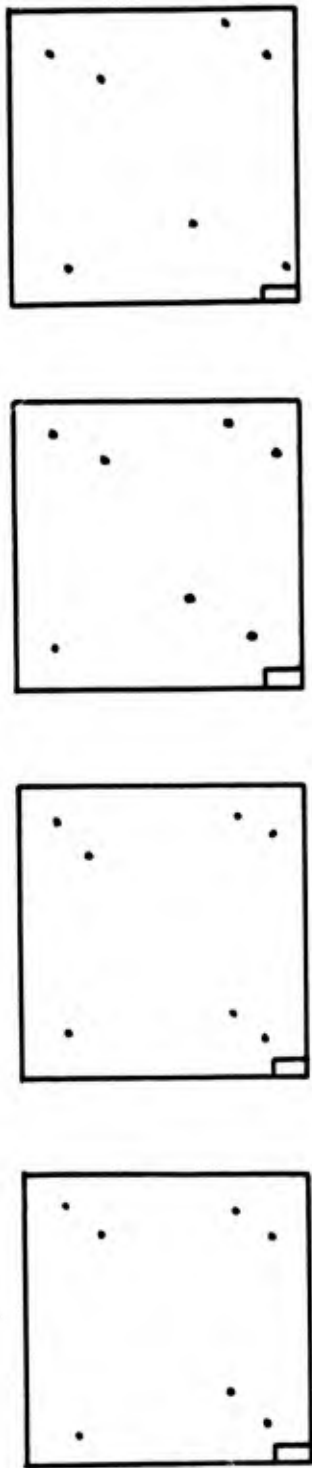
from each of the four flight tracks. Subsequent study of the photography indicated that there were six frames which had ideal target image locations; but unfortunately, they all were taken from the west to east flights. This was of course disappointing and no doubt accounts for some of the degrading of the geometry of the live test when compared to the synthetic data test. In this connection, recommendations will be made for improving the probability of obtaining useful photos on each pass over the Mt. Graham range. The problem is not necessarily one of navigation but of target groupings. Restricting navigation to visual methods is feasible and is in keeping with the guidelines of providing a completely passive calibration range. The limited but well-defined pattern of roads on Mt. Graham made it a simple matter to identify well defined features on flight tracks passing the center of the target field. In fact, a great number of otherwise useful frames were rejected by near misses of only several hundred feet.

The answer seems to lie in the need for additional targets inboard and outboard the prime target locations. In this way, the always present several hundred feet of navigation error (or off verticality) will be absorbed by selection of the alternative images. A greater number of targets is then available but not of particular value geometrically in that they will be closely grouped with other target images.

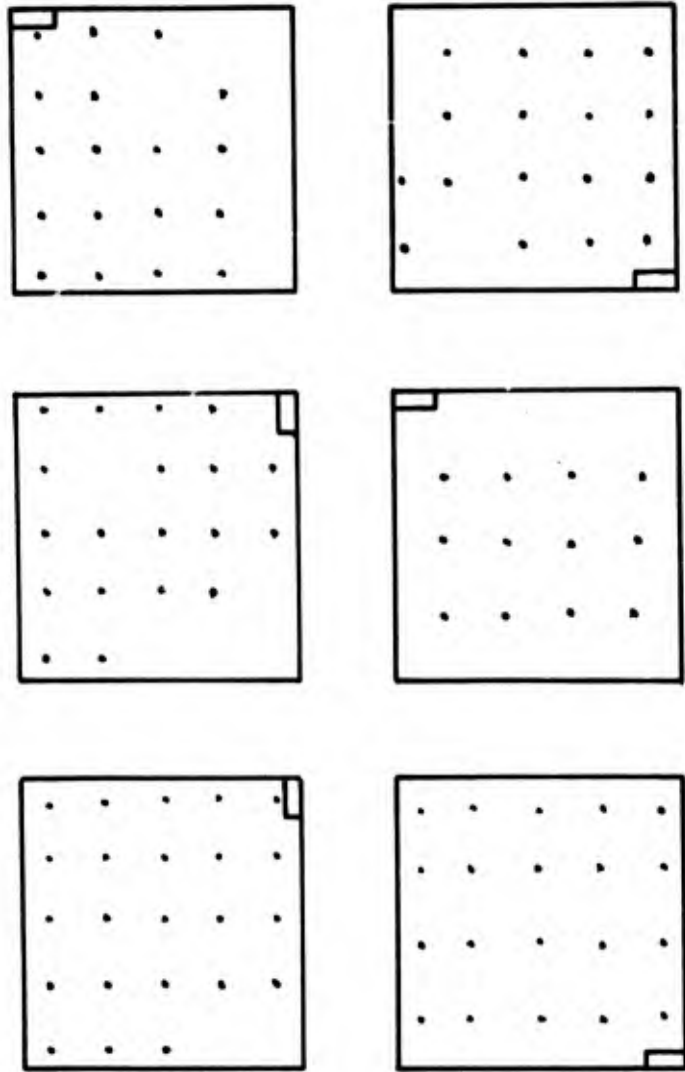
#### 3.6.2.1 Photo Coordinates

The distribution of target images is indicated in Figure 3.6 for each exposure used in the adjustment. The accumulated target image distributions for photography of Mt. Graham and separately for Casa Grande are indicated in Figure 3.7.

Some discussions have been presented regarding results of pre-processing photo coordinate observations. In Section 3.5, the precision of pointing on Mt. Graham targets was given as 2.7 micrometers for a single observation and 6.7 micrometers for Casa Grande. In Section 3.6.1.1, the unit standard error

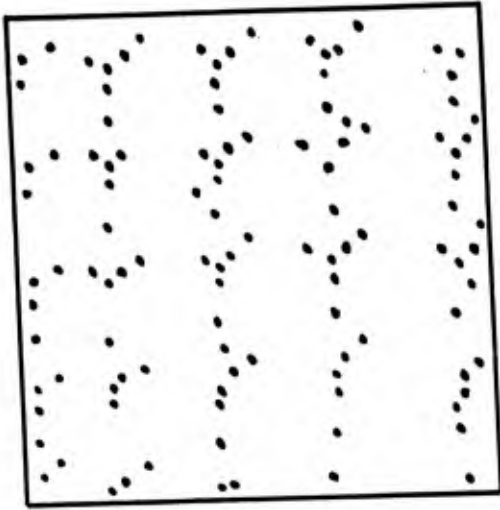


Mt. Graham

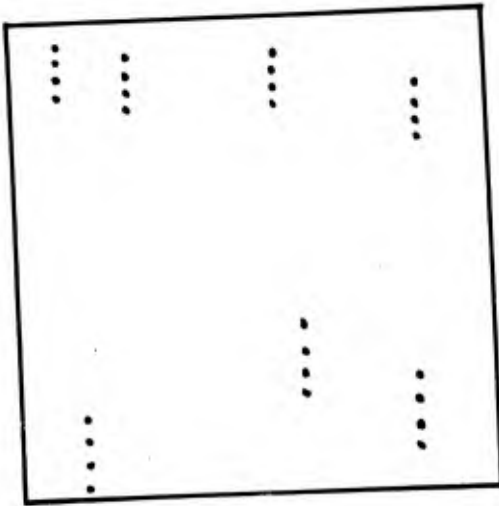


Casa Grande

Figure 3.6 Nominal Target Image Locations on Individual Photographs



Casa Grande



Mt. Graham

Figure 3.7 Cumulative Nominal Target Image Locations on Individual Range Photography

of the fit of the affine model to the four bracketing reseau images averaged 2.7 micrometers showing no significant difference for both ranges.

The final photo coordinate residuals are presented in Table 3.13 in terms of rms errors after the MMR adjustment. There appears to be good consistency between results within a given range. As would be expected, the residuals from Casa Grande were significantly larger; a fact which can be directly attributable to the unfavorable targets at Casa Grande for use with large scale photography.

The marked differences between results at the two ranges cannot be totally explained by comparisons of image quality between the two ranges since the mean value of four repeated observations was used on each target image. Assuming that image quality produces only random pointing errors, the coordinate's observational accuracies became 1.4 and 3.4 micrometers for Mt. Graham and Casa Grande respectively.

A second factor existed which could have introduced a strong systematic influence on the results as evidenced by the disparity between the precision of photo coordinate observations and the fit of these observations to the finally adopted model. Reference is made to the rms errors presented in Table 3.13. Photography of Casa Grande was taken during the reconnaissance flight in May, 1971. The image of targets during this earlier flight appeared in general to be better defined than those of the calibration photography taken in July, 1971. During the week prior to the calibration flight, some dust storms had passed over the Casa Grande area. A little speculation leads to the suggestion that the Casa Grande targets were reduced in contrast by a dust covering and indeed may have in effect been biased in apparent position as well. This is quite reasonable when considering that only the central edges of the wings of the cross formed the useable portions of the Casa Grande targets for this relatively large scale photography.

Mt. Graham	Exposure No.	No. of Targets	rms <sup>x</sup> (micrometers)	rms <sup>y</sup>
	1	7	3.9	2.2
	4	7	4.4	5.4
	8	7	4.6	3.1
	9	7	4.1	1.9
Component Average			4.25	3.15
Group Average			3.70	
Casa Grande				
	2	23	4.5	5.1
	3	19	4.9	5.6
	5	18	5.8	6.4
	6	20	6.5	5.9
	7	12	7.2	4.9
	10	17	3.7	5.1
Component Average			5.43	5.50
Group Average			5.47	
Overall Average			5.11	

Table 3.13 Photocoordinate Residuals After Adjustment (rms) in Micrometers

The presence of unmodeled systematic influences on target coordinate values can not be properly accounted for by choice of weights. These systematic error influences were imposed on the total results of the adjustment. They could reasonably have accounted for the discrepancy on Casa Grande as well as Mt. Graham photography between pointing precision and fit of photo coordinate observations after adjustment. The possible unmodeled bias of only a few centimeters of some of the Casa Grande targets could have also accounted for the unacceptably large unit variance a posteriori of 1.73 as indicated in Table 3.11.

Aside from this problem, there was still a remarkably good agreement between the group average coordinate residuals for Mt. Graham photography and the results reported by Brown [1969] for the KC-6A camera of the USQ-28 Geodetic Sub-System. His results indicated rms residuals after adjustment by SMAC of 3.3 and 3.7 micrometers from two tests; whereas, the results over Mt. Graham, even though contaminated by Casa Grande, showed a rms of residuals of 3.7 micrometers. Brown proceeded to improve upon his result by judicious remodeling or otherwise accounting for persistent systematic errors.

#### 3.6.2.2 Comparison of Results

The results of the adjustment by the MMR and by the laboratory calibration procedures are presented in Table 3.14. The discrepancy between values assigned for the coordinate of the principal point in the x direction could be safely regarded as insignificant. The discrepancy between camera constants (c) could to some extent, but not totally, be explained by the high correlation coefficient between the camera constant and the exposure station elevation coordinate indicated in Table 3.15. Finally, the 146 micrometer discrepancy between values assigned for the y coordinate of the principal point could in no way be explained by its standard error a posteriori nor by its correlation to any other element of interior or exterior orientation. It represented a clear physical disparity between the two calibration procedures.

Unconstrained Parameters (interior orientation)	MMR Results		Laboratory Results	
	adjusted values	std. error	adopted values	std. errors
$x_0$ (mm)	0.009	0.017	0.00	0.030 *
$y_0$ (mm)	0.146	0.023	0.00	0.030
$c$ (mm)	-152.239	0.027	-152.01	0.030 **
K1	$-0.72265 \times 10^{-7}$	$0.171 \times 10^{-7}$	---	---
K2	$+0.67113 \times 10^{-11}$	$0.149 \times 10^{-11}$	---	---
K3	$-0.15912 \times 10^{-15}$	$0.387 \times 10^{-16}$	---	---
P1	$-0.57143 \times 10^{-6}$	$0.133 \times 10^{-6}$	---	---
P2	$-0.41770 \times 10^{-6}$	$0.142 \times 10^{-6}$	---	---

\*\* [Zeiss, 1968] -- "The probable errors of these determinations do not exceed +0.02mm."

\* [Zeiss, 1968] -- "The lines joining opposite pairs of fiducial markers intersect an angle of  $90^{\circ} \pm 30$  seconds. Their intersection indicates the location of the principal point of autocollimation with an accuracy of +0.02mm" -- taken here also as a probable error.

Table 3.14 Results of the MMR Adjustment and of the Laboratory Calibration for the RMK-AR 15/23 Serial No. 21 197

	$x_o$	$y_o$	$z_o$	$\phi$	$\omega$
Typical of					
Mt. Graham	.49	.23	.25	-.62	.08
photo No. 1					
	.47	.66	-.36	-.31	.19
	.35	.31	-.93	.34	.04
Typical of					
Casa Grande	-.66	-.37	.17	.08	-.09
photo No. 7					
	.39	-.76	.38	-.02	-.13
	.75	-.32	-.93	-.03	+.02

Table 3.15 Typical Values of Correlation Coefficients Relating Selected Sensitive Elements of Interior and Exterior Orientation

It is interesting to note that a similar unexplained shift of the principal point coordinate in the y direction occurred for the KC-6A camera in the McClure, Ohio test [Brown, 1969]. In that case, a value of about 100 micrometers was computed for the shift. In the present experiment, it is recalled that the camera was installed in a single radial engine aircraft (Cessna 195). The view of the camera was through the turbulent (non-laminar) region generated not only by the slip stream from the propeller but also by the cooling air after passing the cowling. The results of ray tracing through such a volume of turbulence in an effort to account for the shift of the principal point would be clouded by the necessary assumptions generalizing its physical state.

In most applications of aerial photogrammetry, the affect of the neglect of the systematic discrepancies for values of camera constant and principal point coordinates may be effectively suppressed by projective compensation. However, there are three distinct cases in which the process of projective compensation does not fully account for these errors of interior orientation (the first two have been discussed by Brown [1969]):

1. observations made on some or all of the elements of exterior orientation (examples: USQ-28, Apollo SIM)
2. adjusted values of exterior orientation used as standards of comparison for positional or orientational sensors (examples: vertically stabilized mounts, SHIRAN, ASFIR)
3. mapping or aerial triangulation over mountainous regions or under circumstances in which variation in the object distance approaches a significant portion of the total object distance

The neglect of proper system calibration for applications within these three categories could seriously compromise the photogrammetric procedure.

To illustrate case 2, two photographs taken over the Casa Grande range were used to compare adjusted values of exterior orientation. These photographs were not used in the MMR adjustment but were taken on the same flight

mission. A single photo resection was computed using first the laboratory values then the MMR values of interior orientation for each photo. The differences in computed values of exterior orientation are presented in Table 3.16. The second differences indicate the stability of the photogrammetric resection for the selected locations of targets as well as the persistency of the influence of the two calibration procedures.

Figure 3.8 presents a graphical comparison of distortion determined by laboratory and MMR procedures. The physical interpretation of the differences between the two procedures is difficult by such direct comparisons. A more meaningful comparison would be obtained when applied to all of the three non-projectively compensated cases described earlier.

Exterior Orientation Parameter	Laboratory Calibration - MMR		Second Differences $\Delta' - \Delta''$
	$\Delta'$ (Photo 166)	$\Delta''$ (Photo 167)	
$\kappa$ (arc sec.)	-4	-2	-2
$\varphi$ (arc sec.)	-58	-66	+7
$\omega$ (arc sec.)	+29	+17	+12
$X_o$ (meters)	-0.84	-0.97	+0.13
$Y_o$ (meters)	+3.91	+4.21	-0.30
$Z_o$ (meters)	-6.66	-6.62	-0.04

Table 3.16 Differences in Results for Exterior Orientation After Single Photo Resections When Using Interior Orientations Determined by Laboratory and MMR Procedures (terrain clearance about 16,000 feet)

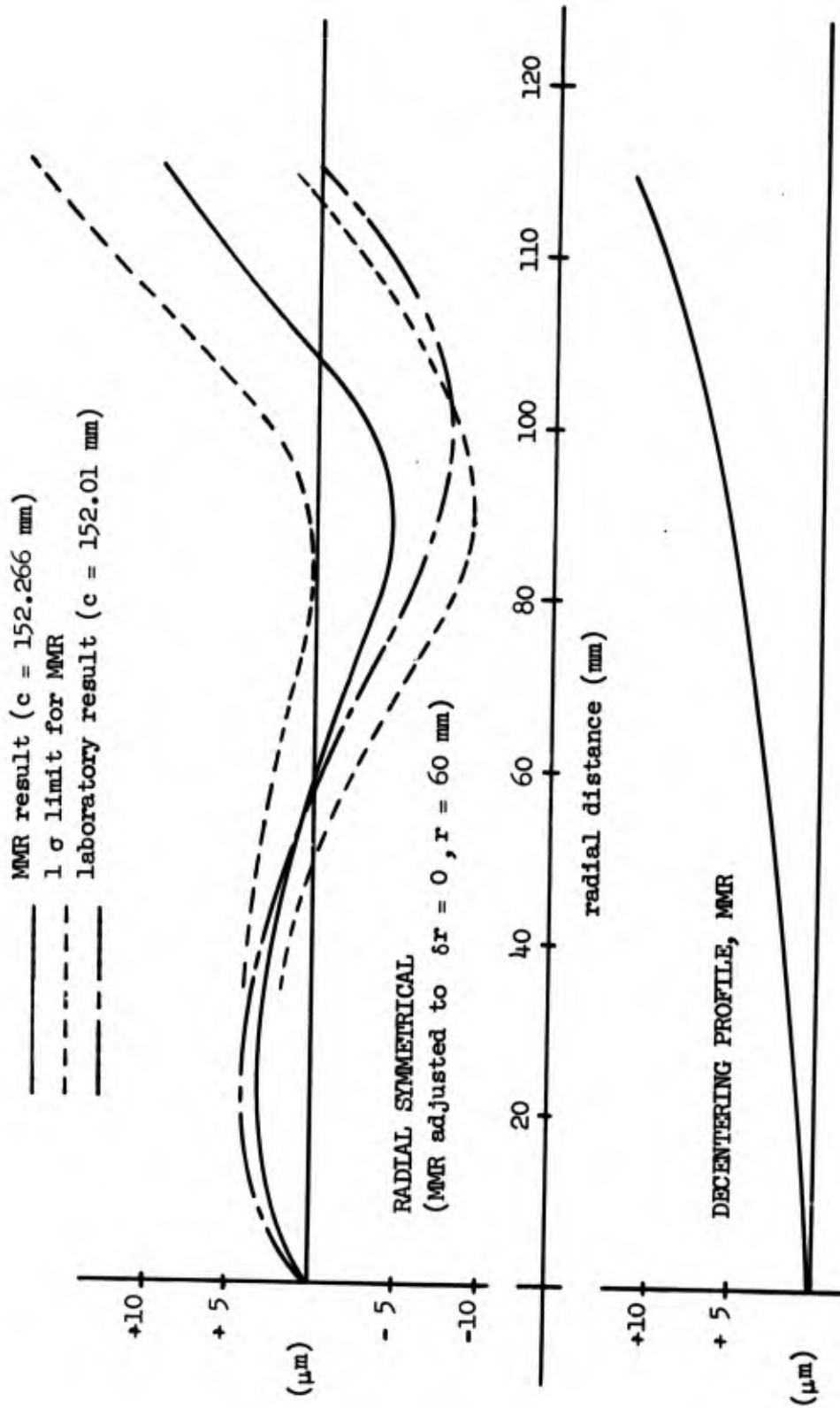


Figure 3.8 Distortion Determined by MMR and Laboratory Procedures

#### 4. Conclusions and Recommendations

This report has discussed the theory and results of a demonstration of the MMR procedure for conducting the calibration of the aerial photographic system. When compared to previous experiments, this procedure conforms most closely to Eisenhart's [1963] concept of calibration. The goal of this research was not to demonstrate more precise results than have heretofore been attained; but rather, to demonstrate that the MMR procedure can be feasibly conducted in a cost-effective manner which would lead to reliable results for those metric quantities which define the operational photographic system. It is concluded that this goal has been attained.

Sufficient experience is not available to confidently predict the metric effectiveness of a specific aerial photographic system. However, the results of this research in which the observations of photo coordinates agreed with the adopted model with an rms error of 5.1 micrometers offer strong evidence that the MMR procedure would be effective as a means for establishing and maintaining calibration for the aerial photographic system. From an effectiveness point of view, there has been only one other experiment with the aerial photographic system which is not considered deficient. The work with the KC-6A camera over the McClure Camera Calibration Range is certainly a most effective procedure [Brown, 1968]. The expected cost of the MMR procedure would include estimates for acquisition of range photography, coordinate observations and data reduction. These costs would occur each time the aerial system is sampled in an on-going program of calibration but would not include those for establishing a mountain range (or other suitable 3-dimensional range), or maintenance of the ranges. Photography acquisition costs would vary depending on proximity to the ranges. The data processing should not exceed 20 man days for a ten photo sample. Computer costs would be relatively negligible. In a production mode, the man hours required could drop considerably. Such costs are modest when compared to anticipated improvements in

effectiveness; particularly for those critical applications in which exterior orientation is important or over significantly three-dimensional terrain. The MMR procedure is offered as an outstanding cost-effective candidate for the calibration of the aerial photographic system.

Several distinct problems arose during the course of the research. The quality of the target images on the relatively large scale Casa Grande photography introduced some significantly large influences on the adjustment. Images of Mt. Graham targets permitted a standard pointing error of 2.7 micrometers; whereas, for Casa Grande, the value was 6.7 micrometers. Although the mean of four observations on each image was used, the relatively poor Casa Grande imagery no doubt accounts to a large extent for the disparity between the precision of observations and the rms of the residuals after adjustment (Mt. Graham rms of 3.7 and Casa Grande rms of 5.5 micrometers).

A second aspect of the MMR as revealed by this investigation is the need for some additional strengthening of the geometry of the three-dimensional range to further suppress the high correlation between the camera constant and the elevation coordinate of the exposure station. The remaining correlations between  $(x_0 \text{ to } X_0)$  and  $(y_0 \text{ to } Y_0)$  were sufficiently suppressed.

A prime example of the potential failure of calibration of system components alone for subsequent representation of the total operational system is provided by the significant difference in the value obtained for the y coordinate of the principal point. Only by rational sampling of the total operating system can reasonable assurance be offered that such systematic influences are taken into account.

The first recommendation is that a selected region of the Casa Grande range be improved by altering the center section of the existing targets. The new targets would make the Casa Grande range useful for the broad range of normally aspirated aircraft. The use of the range could also then be extended to a relatively low altitude calibration procedure for all aerial photographic

systems. The improvements would be accomplished by filling the ten foot void at the existing target center with a flat black background. A circular flat white target would then be centered on the station. If it is assumed that the targets are to be designed for photography from a six inch focal length camera at 20,000 feet, then the target circle diameter should be about six feet. The resulting image diameter would be about 50 micrometers. The alterations need be accomplished only over a 6 by 6 array of targets. Further random densification would be desirable but would be relatively expensive as compared to the slight modifications to the existing targets as recommended. Also, recommended in this connection is a continual maintenance program to assure that the targets are reasonably clear from dust, sand, or weed cover.

The primary recommendation is that an aerial photographic system calibration program be instituted on a pilot basis. The procedure would be that of MMR. The periodic reapplication of this procedure coupled with a continuing analysis of system performance by techniques similar to those of statistical process control would produce the first aerial photographic system in full accord with Eisenhart's concept of system calibration. The KC-6A camera, suitably installed in a representative photo aircraft, would constitute the major component of the aerial photographic system. Alterations to 36 of the Casa Grande targets as discussed earlier would be required. Some additional surveys on the south edge of the Mt. Graham range would be desirable to extend station C to a lower elevation. A one year program of bimonthly sampling would clearly establish the procedure and would offer reasonable assurance that a state of statistical control would be established. This program would demonstrate the final phase of calibration for the aerial photographic system. It would remain then only to institute a continuing program for establishing and maintaining the calibration of those aerial photographic systems for which high accuracy or other special applications are intended.

## References

- American Society of Photogrammetry (1966) "Manual of Photogrammetry, 3rd Ed." A.S.P., 6269 Leesburg Pike, Falls Church, Virginia, 1966.
- Bender, Lee U. (1971) "Analytical Photogrammetry, A Collinear Theory" RADC-TR-71-147, August, 1971.
- Brown, D. (1964) "An Advanced Reduction and Calibration for Photogrammetric Cameras" Instrument Corp. of Florida, 10 Jan. 1964.
- Brown, D. (1965) "Decentering Distortion and the Definitive Calibration of Metric Cameras" presented at the A.S.P. Convention, March 1965.
- Brown, D. (1966) "Decentering Distortion of Lenses" Photogrammetric Engineering, Vol. XXXII, No. 3.
- Brown, D. (1969) "Advanced Methods for the Calibration of Metric Cameras" paper presented at Symposium on Computational Photogrammetry at Syracuse University, College of Forestry, Jan., 1969.
- Brown, D, Davis, R, Johnson, F (1964) "Research in Mathematical Targeting" RADC-TDR-64-353 Oct., 1964.
- Conrady, Prof. A. E. (1919) "Decentered Lens Systems" Monthly Notices of the Royal Astronomical Society, Vol. 79, pp. 384-390, 1919.
- Eisenhart, Churchill (1963) "Realistic Evaluation of the Precision and Accuracy of Instrument Calibration Systems" Journal of Research of The National Bureau of Standards - C. Engineering and Instrumentation, Vol. 67, C. No. 2 April - June 1963.
- Jeyapalan, K. (1972) "Dynamic Calibration of Cameras and its Effect on Block Triangulation" University of London, Dissertation, approval and publication pending.
- Kodak (1965) "Manual of Physical Properties, Aerial and Special Materials" Eastman Kodak Co., Rochester, N. Y., 1965.
- Merchant, Dean C. (1967) "Calibration of the Aerial Photographic System" Dept. of Geodetic Science, The Ohio State University (dissertation) June, 1967.

- Merchant, Dean (1968) "Calibration of the Aerial Photographic System" Rome Air Development Center, TDR-68, 1968.
- Merchant, Dean C. (1971) "An Investigation Into Dynamic Aerial Photographic System Calibration" RADC-TR-71-174, Final Technical Report, August 1971.
- Moren, A. "The Geometrical Quality of the Aerial Photographs" Thesis, Royal Institute of Technology, Stockholm, Div. of Photogrammetry, 1967.
- Pope, Allen J. (1972) "Some Pitfalls to be Avoided in the Iterative Adjustment of Nonlinear Problems" Proceedings of the 38th Annual Meeting, American Society of Photogrammetry, March 12-17, 1972.
- USAE (1968) "Specifications for Monument Markers at Casa Grande Test Range, Casa Grande, Arizona" DACA 09-69-B-0026, U.S. Army Engineer District, Los Angeles, Corps of Engineers, 28 August 1968.
- Ziemann, H. (1968) "Reseau Photography in Photogrammetry" National Research Council of Canada, 1968.
- Zeiss (1968) "Inspection Slip for Photogrammetric Lenses, RMK-AR 15/23 No. 21 197" Carl Zeiss, Oberkochen, Sept. 10, 1968.

Appendix A

The Zeiss Calibration Report for  
 RMK-AR 15/23 No. 21 197  
 [Zeiss, 1968]

The lens Pleogon Ar maximum aperture  $f/5.6$   
 nominal focal length 153 mm, serial no.: 98 222

has been inspected in accordance with the existing regulations. The optical performance and the external construction are in accordance with our terms of delivery.

I. Focal length

Equivalent focal length =  $\infty$ .

Calibrated focal length = 152.01

The probable errors of these determinations do not exceed  $\pm 0.02$  mm.

II. Distortion

in 4 Semi-Diagonals referring to the  
 Point of Autocollimation

mm	0	10	20	30	40	50	60	70	80	90	100	110	120	130	140	150	
I	A	0	-4	-6	-6	-4	-3	-1	+2	+8	+8	+4	+2	+6	+9	+3	./.
	B	0	-4	-5	-6	-3	0	+2	+6	+8	+7	+3	+6	+7	+5	-1	./.
II	C	0	-4	-4	-6	-3	-3	0	+5	+5	+5	+5	+3	+6	+8	+2	./.
	D	0	-3	-5	-5	-2	-1	+2	+6	+8	+8	+5	+3	+7	+7	-3	./.
Average		0	-4	-5	-6	-3	-2	+1	+5	+7	+7	+4	+4	+7	+7	0	./.

The values of distortion base upon calibrated focal length. They are determined for points separated by 10 mm from the axis for each of the four radii and given in microns. They indicate the displacement of the image from its distortion-free position. A positive value indicates a displacement away

from the centre Measurements were made at aperture  $f/5.6$  on the goniometer by attaching the filter D (transmittance limit 520 nm) with an accuracy of  $\pm 0.002$  mm.

### III. Photographic Resolving Power

The photographic resolution was obtained in accordance with the recommendations of the International Society of Photogrammetry. The contrast of the 3 line test figures of the prescription on dark background was (in logarithmic scale) 1.6. The following emulsion was used as taking material:

Perutz - Pervola  
with a speed of  $20^{\circ}$  DIN. The developer used was  
Perufin

The photographs were taken under the recommended standard illumination by using the filter B (transmittance limit 470 nm) in parallel light. The following values were obtained for the aperture ration  $f/5.6$  for radial and tangential image elements in lines/mm and reduced to the image plane. They refer to the given nominal focal length.

Image angle: $W =$	$0^{\circ}$	$7^{\circ}$	$14^{\circ}$	$21^{\circ}$	$28^{\circ}$	$35^{\circ}$	$42^{\circ}$
Resolution radial	60	50	47	37	30	30	27
Resolution tangential	60	47	40	35	28	24	15

### IV. Principal Point of Autocollimation

The lines joining opposite pairs of fiducial markers intersect an angle of  $90^{\circ} \pm 30^{\circ}$  seconds. Their intersection indicates the location of the principal point of autocollimation with an accuracy of  $\pm 0.02$  mm.

### V. Fiducial marker separation

$$x = 226,004$$

$$y = 226,008$$

$x$  lies in the flightline. The values have been determined with an accuracy

of  $\pm 0.02$  mm.

#### VI. Tangential Distortion

The maximum tangential distortion, that means the displacement of the central image from a straight line connecting corresponding image points at equal but opposite angular separations from the axis, does not exceed 10 microns.

#### VII. Filters

The two surfaces of the filters

K (clear)	no: 15 438
B (yellow)	no: 14 480
D (orange)	no: 15 497

are parallel to within 5 seconds of arc.

#### VIII. Magazine Platen

The platen mounted in Zeiss-Magazine Type FK 24/120 no.: 11 00 26 does not depart from a true plane by more than  $\pm 0.010$  mm.

CARL ZEISS

Photogrammetric Department  
i.A.

Oberkochen, the September 10, 1968

According to inspection slip  
dtd. July 18, 1968

Pti/PM

## Appendix B

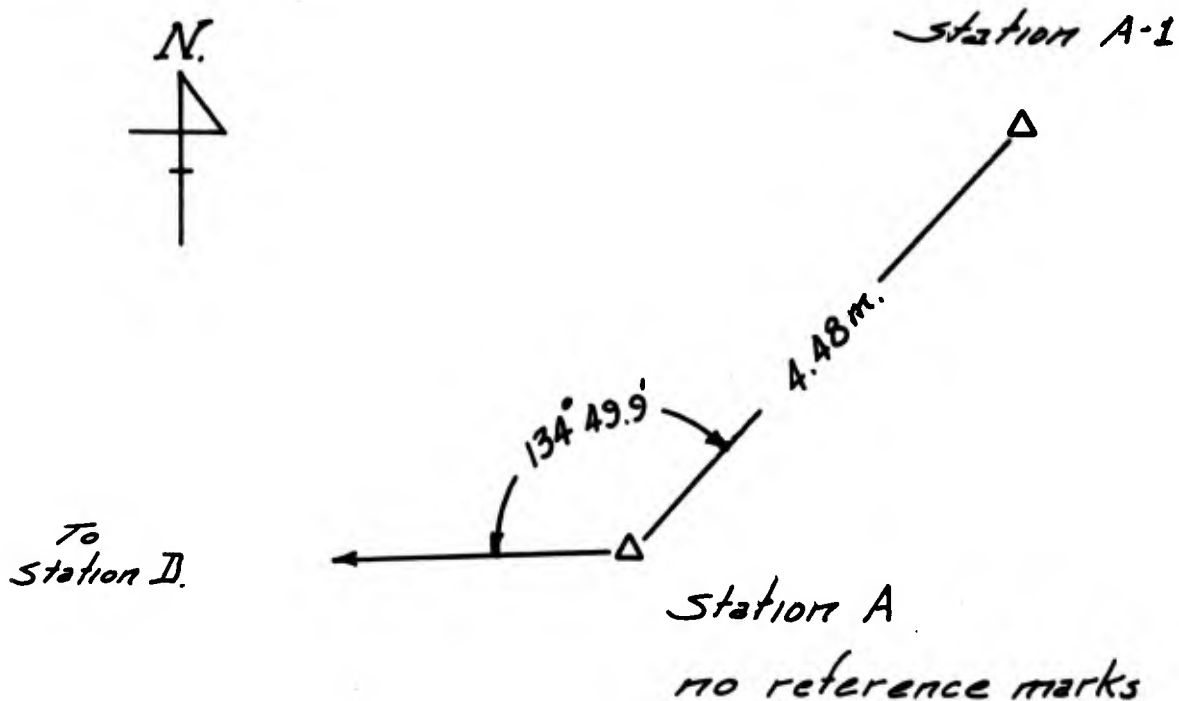
### Station Descriptions, Mt. Graham Calibration Range Survey

These station descriptions prepared by Mr. Sol Cushman describe both the primary stations of the horizontal and vertical geodetic surveys and also the off-set stations on which additional targets were located. The additional targets were in all cases located only a few meters from the primary stations. These additional targets were used at all stations with the exceptions of station (F) and (H).

(Note: References to page numbers are with respect to Field Book 3207-A1)

**Preceding page blank**

Near Milepost 124 Swift Trail. Access by climbing rock cliff (10 feet) thence 150 feet to station. Station is a  $\frac{1}{4}$ -inch hole drilled in rock near south end of rock out crop. Station A1 is also a  $\frac{1}{4}$ -inch hole drilled in a rock NNE of A. (Pages 2, 8c, 4)



Distance A to A1 = 4.48 meters (Page 4)

Direction at A: D to A1 =  $134^{\circ} 49.9'$  (Page 17)

Difference of Elevation: A to A1 = +0.25 feet (Page 4)

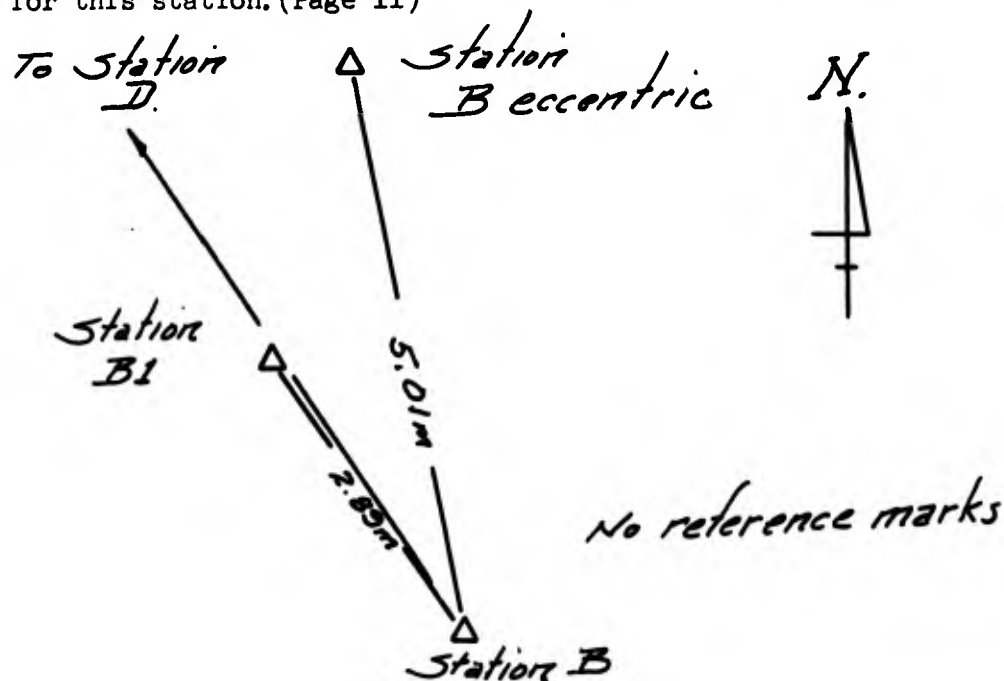
Elevation of Station A = 6214.8 feet (Page 60)

All occupations of A for horizontal angles and double zenith distances were without eccentricity.

All observations of A for horizontal angles were without eccentricity.

Observations of A for double zenith distances were without eccentricity from B; eccentric target shown to D is described on Page 36, station A1 was not occupied.

Near Milepost 134 Swift Trail. Ascend either of two draws near milepost to foot of rock outcrop. Ascend draw near SE end of outcrop to ridge covered with scrub oak, turn left (northwest) and ascend rock to station set in hollow top of SE end of outcrop. Station is marked by a five inch chrome plated centerpunch driven flush in rock. Station B1 was marked temporarily during photography but no longer exists. Station B eccentric is marked by a chiselled cross on surface of rock. Small holes for tripod feet have been chiselled for this station. (Page 11)



Distances (horizontal) B to B1 = 2.89 meters (Page 11)

B to B ecc = 5.01 meters (Page 24)

Approx. horizontal angles at B: to D =  $0^{\circ} 00'$

to B ecc =  $22^{\circ} 42'$  (Page 25 8c Computations)

to B1 =  $359^{\circ} 11'$  (Page 10 but see Page 25)

Diff. of Elevations: B to B1 = -0.26 meters (Page 11)

B to B ecc = +4.0 inches (Page 25)

Station B1 was not occupied.

Station B had no eccentricities of either occupation or observation.

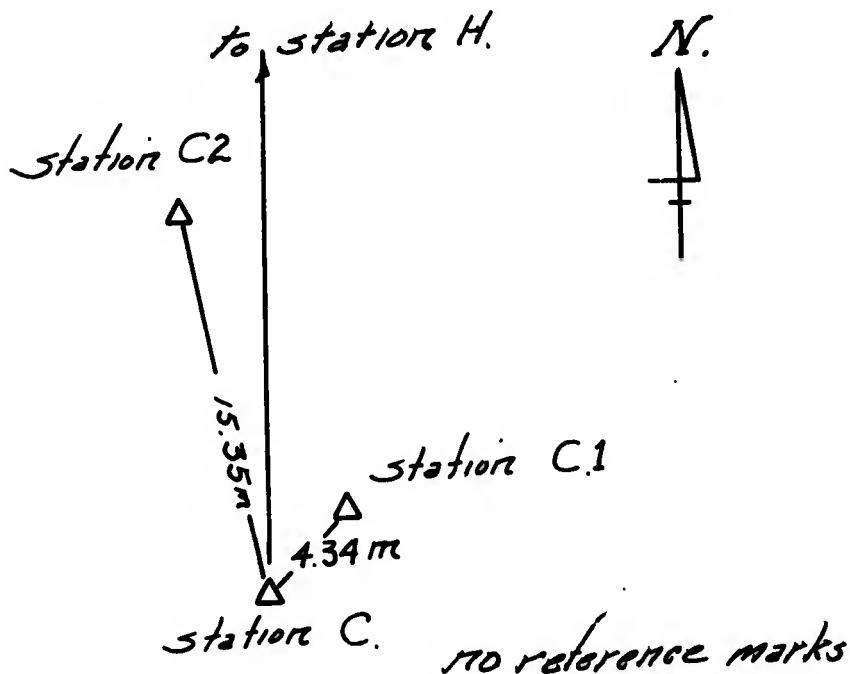
Station B ecc was occupied and observed in connection with ties to station

G, only.

Station Descriptions (Station C)

Mt. Graham Survey

Near Milepost 133.3 descend narrow ridge SE through second pine forest to rocky area. Station is a cross chiselled on upper surface of large boulder (lower and easterly of two). Stations C1 and C2 were marked during photography only and no longer exist. (Page 5)



Distances: C - C1 = 4.34 meters (Pages 5 and 217)

C - C2 = 15.35 meters (Pages 5 and 217)

Horiz. Directions at C: To H =  $0^{\circ} - 00'$

To C1 =  $42^{\circ} - 02'$  (Page 217)

To C2 =  $345^{\circ} - 54'$  (Page 217)

Differences of Elevation: C to C1 = - 2.48 meters (Page 217)

C to C2 = + 0.82 meter

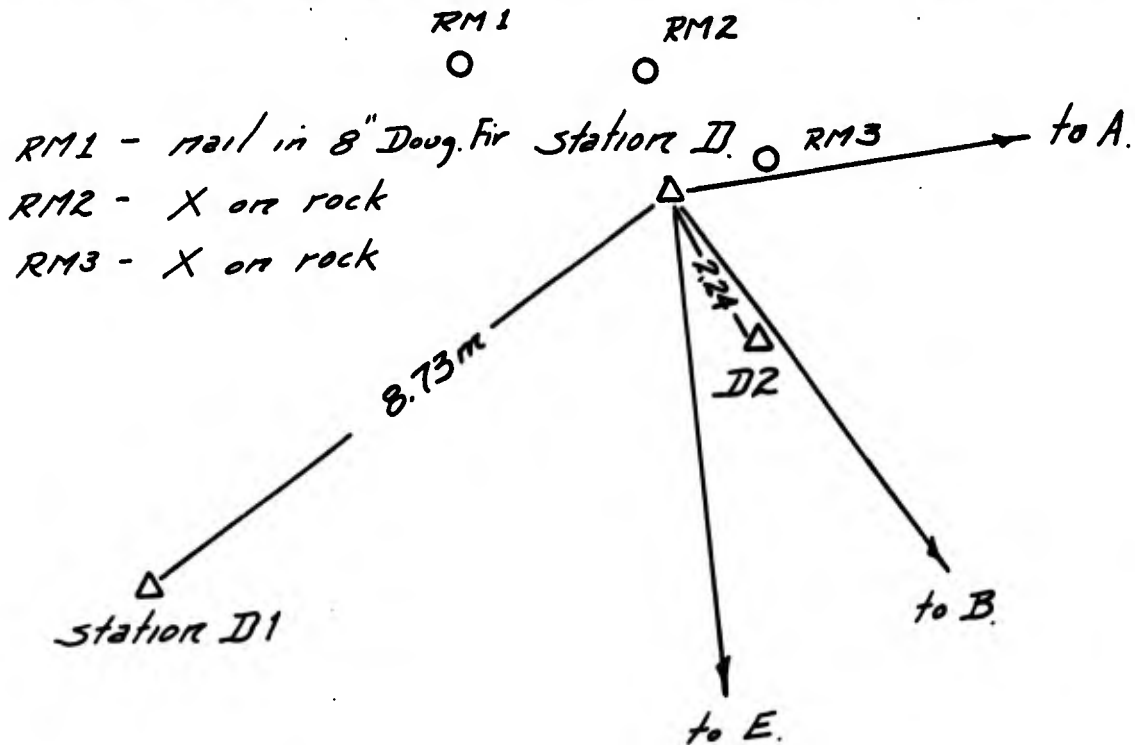
All occupations and observations at C are without any eccentricities.

Stations C1 and C2 were not occupied.

Station Descriptions (Station D)

Mt. Graham Survey

Near only fork in road to Heliograph Look Out Tower. Leave road at trail marker on east side of road. Follow contour and trail for about three hundred feet, thence, bear left, uphill fifty feet to station at rock outcrop. Station is marked by 2 x 2 inch stake with red tape and cup tack. Stations D1 and D2 were marked temporarily for photography and no longer exist. (Page 8)



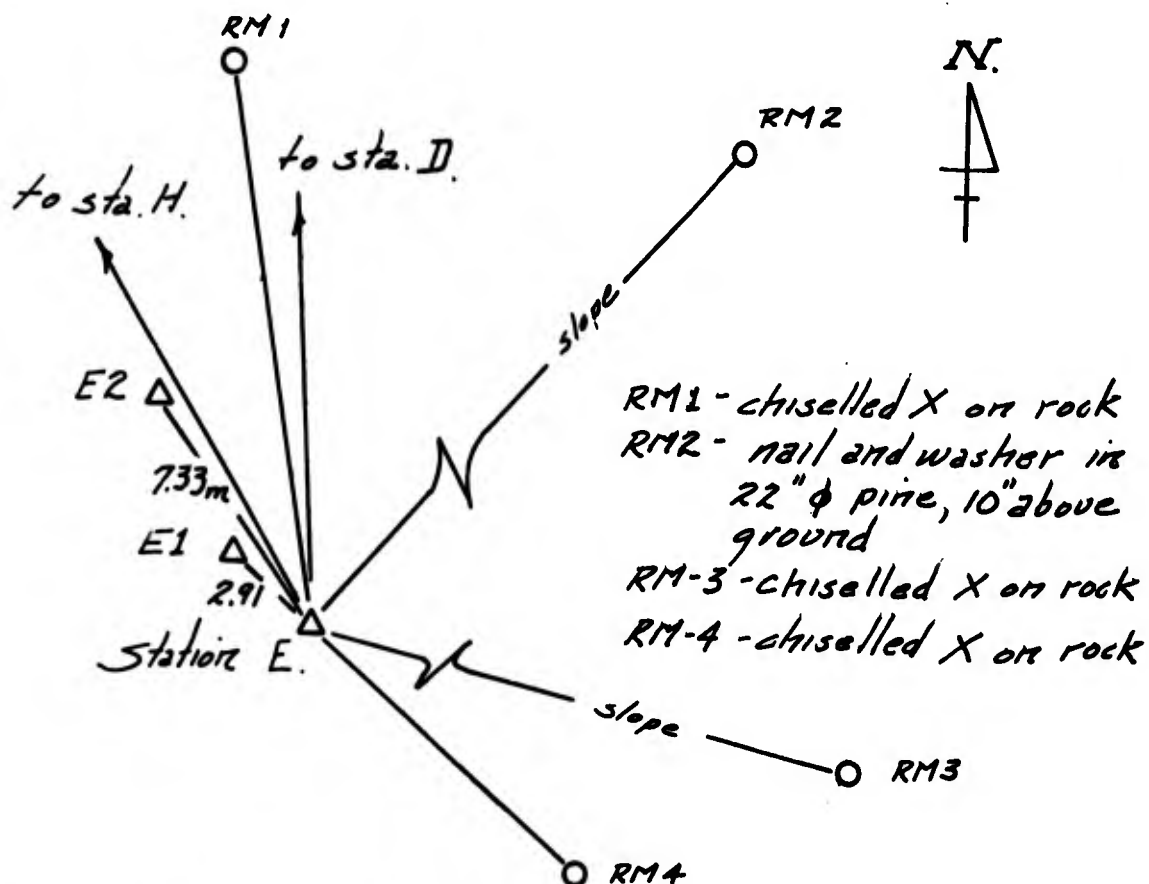
Horizontal distances: D to D1 = 8.73 meters  
 D to D2 = 2.235 meters  
 D to RM1 = 4.507 meters (Page 8)  
 D to RM2 = 1.795 meters  
 D to RM3 = 0.89 meters

Horizontal Directions at D: To F = 0° - 00'  
 To D2 = 54° - 22' (Page 8)  
 To D1 = 137° - 02'

Differences of Elevation: D to D1 = -8.96 feet (Page 8)  
 D to D2 = -1.22 feet

No eccentricities of occupation or observation except during double zenith distances to and from A. Eccentric target Page 32.

Near milepost 133.6 on Swift Trail on west edge of roadway. Stations E, E1, and E2 are each marked by 2 x 2 inch stakes with red tape and cup tacks. All are likely to be destroyed in scheduled and frequent regrading of road bed. (Page 13)



Horizontal distances: E to E1 = 2.91 meters  
 E to E2 = 7.33 meters  
 E1 to E2 = 4.61 meters  
 E to RM1 = 23.29 meters  
 E to RM4 = 9.52 meters

Slope distances: E to RM2 = 16.87 meters  
 E to RM3 = 14.90 meters

Horizontal Directions at E: to H = 0° 00'  
 to E1 = 340° 04'  
 to E2 = 356° 35'

(Page 13)

Station Descriptions (Station E)

Page 2

Differences of elevation: E to E1 = -0.06 foot  
E to E2 = -0.30 foot  
E to E1hub = -2.35 feet  
E to E2hub = -2.51 feet  
E to RM1 = +5.30 feet  
E to RM2 = +2.21 feet

(Page 13)

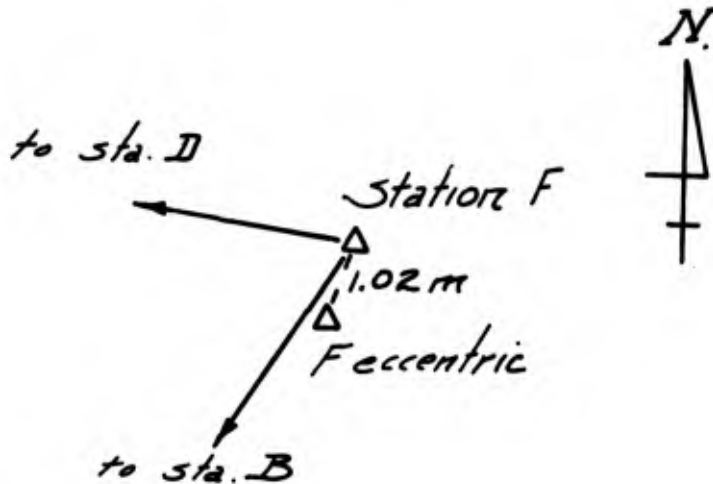
Note: hubs for E1 and E2 were located below targets for photography.  
No eccentric observations or occupations are involved at this station.

Stations E1 and E2 were not occupied.

Station Descriptions (Station F)

Mt. Graham Survey

Near Milepost 126.3 on Swift Trail, on large rock overhanging north side of road approximately one hundred feet east of side road to orchard. Station F is marked by a drill hole on top of rock, and station F eccentric is marked by a cross chiselled on same rock. (Page 20)



*NO reference marks*

Horizontal distance F to F eccentric = 1.02 meters (Page 20).  
 Horizontal angle at F<sup>ecc</sup> between D and F = 106° 13' (Page 19)  
 Difference in elevation: F to F<sub>ecc</sub> = +3.0 inches (Page 61)

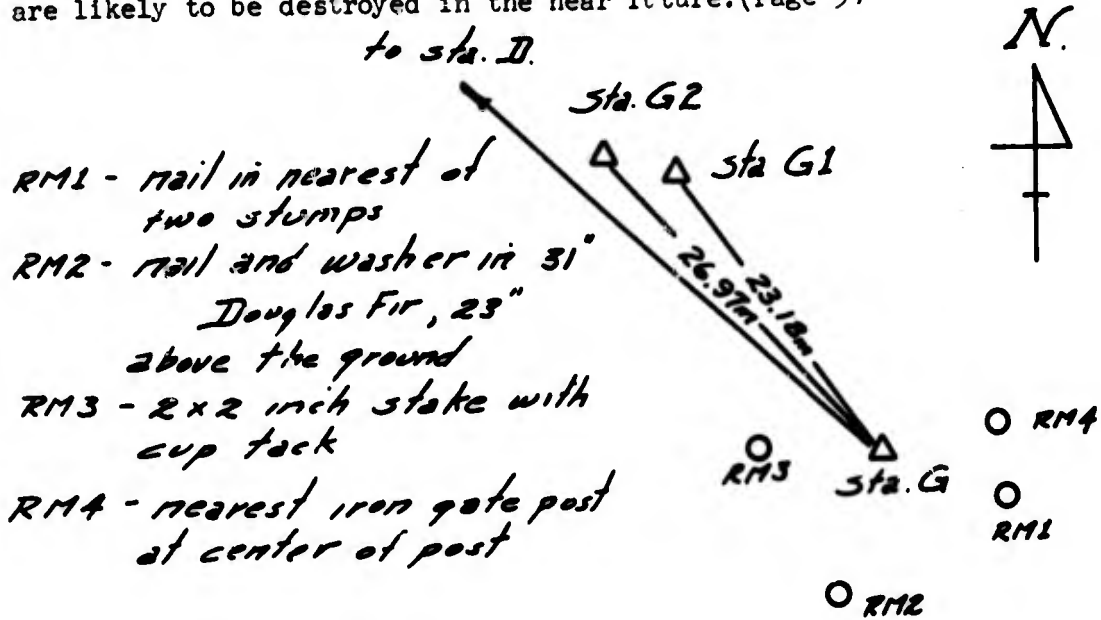
All occupations and observations involving this station refer to the eccentric station.

Only one photo target was placed at this station and that on station F.

Station Descriptions (Station G)

Mt. Graham Survey

Near Milepost 128.5 on Swift Trail on south side of junction with new highway. Station is a hole drilled in a large surface boulder. Stations G1 and G2 are marked with 2 x 2 inch stakes with cup tacks. These stations are likely to be destroyed in the near future. (Page 9)



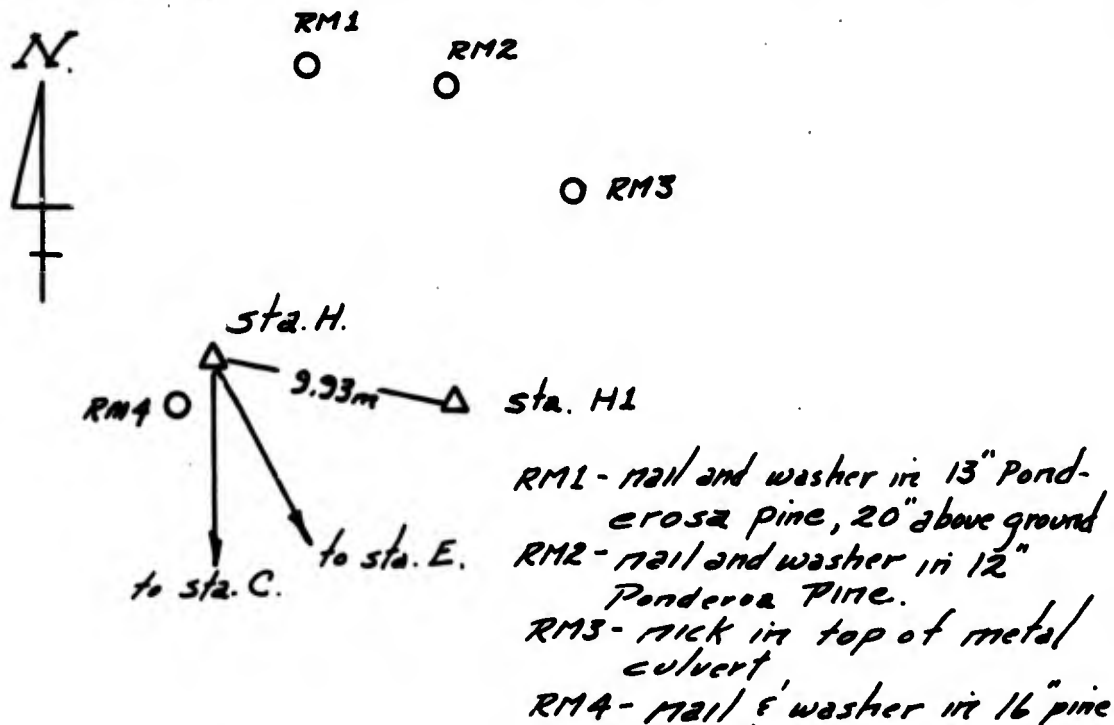
- Horizontal distances:
- G to G1 = 23.18 meters
  - G to G2 = 26.97 meters
  - G1 to G2 = 4.775 meters
  - G to RM1 = 8.47 meters (Page 9)
  - G to RM2 = 9.69 meters
  - G to RM3 = 8.13 meters
  - G to RM4 = 8.03 meters
- Horizontal directions at G:
- to D = 0° - 00' (Page 16)
  - to G2 = 8° - 13'
  - to G1 = 15° - 03'
- Differences in elevation:
- G to G1 = -12.06 feet (Page 16)
  - G to G2 = -10.62 feet

All occupations of and observations to G have been without eccentricities. Stations G1 and G2 were not occupied.

Station Descriptions (Station H)

Mt. Graham Survey

Near Milepost 134.5 on Swift Trail on south side of road. Both stations H and H1 are marked with 2 x 2 inch stakes with red tape and cup tack. Both stations are likely to be destroyed during frequent and regular regrading of road bed. (Page 7)



Horizontal distances: H to H1 = 9.93 meters (Page 12)

H to RM4 = 2.16 meters (Page 7)

Slope distances:

H to RM1 = 17.44 meters

H to RM2 = 20.69 meters (Page 7)

H to RM3 = 24.12 meters

Horizontal directions at H: to E = 0° 00'

to C = 32° 47' (Page 6)

to H1 = 310° 18' (Page 12)

Differences of elevation: H to H1 = -2.05 feet

H to RM3 = -4.61 feet (Page 12)

H to H1hub = -4.48 feet

All occupations of and observations to this stations are without eccentricities.